

# AAPM protocol for 40–300 kV x-ray beam dosimetry in radiotherapy and radiobiology

C.-M. Ma, Chair<sup>a)</sup>

*Radiation Oncology Dept., Stanford University School of Medicine, Stanford, California 94305-5304 and Ionizing Radiation Standards, National Research Council of Canada, Ottawa K1A 0R6, Canada*

C. W. Coffey<sup>b)</sup>

*Department of Radiation Oncology, Vanderbilt Medical Center, B 902 Vanderbilt Clinic, Nashville, Tennessee 37232-5671*

L. A. DeWerd<sup>c)</sup>

*University of Wisconsin, 1530 MSC Medical Physics, 1300 University Avenue, Madison, Wisconsin 53706*

C. Liu<sup>d)</sup>

*Department of Radiation Oncology, University of Florida, Gainesville, Florida 32610-385*

R. Nath<sup>e)</sup>

*Department of Therapeutic Radiology, Yale School of Medicine, 333 Cedar Street, New Haven, Connecticut 06510*

S. M. Seltzer<sup>f)</sup>

*Ionizing Radiation Division, National Institute of Standards and Technology, Gaithersburg, Maryland 20899*

J. P. Seuntjens<sup>g)</sup>

*Medical Physics Unit, McGill University, Montreal General Hospital, 1650 Avenue Cedar, Montréal H3G 1A4, Canada and Ionizing Radiation Standards, National Research Council of Canada, Ottawa K1A 0R6, Canada*

(Received 5 March 2001; accepted for publication 12 March 2001)

The American Association of Physicists in Medicine (AAPM) presents a new protocol, developed by the Radiation Therapy Committee Task Group 61, for reference dosimetry of low- and medium-energy x rays for radiotherapy and radiobiology ( $40 \text{ kV} \leq \text{tube potential} \leq 300 \text{ kV}$ ). It is based on ionization chambers calibrated in air in terms of air kerma. If the point of interest is at or close to the surface, one unified approach over the entire energy range shall be used to determine absorbed dose to water at the surface of a water phantom based on an in-air measurement (the “in-air” method). If the point of interest is at a depth, an in-water measurement at a depth of 2 cm shall be used for tube potentials  $\geq 100 \text{ kV}$  (the “in-phantom” method). The in-phantom method is not recommended for tube potentials  $< 100 \text{ kV}$ . Guidelines are provided to determine the dose at other points in water and the dose at the surface of other biological materials of interest. The protocol is based on an up-to-date data set of basic dosimetry parameters, which produce consistent dose values for the two methods recommended. Estimates of uncertainties on the final dose values are also presented. © 2001 American Association of Physicists in Medicine.

[DOI: 10.1118/1.1374247]

Key words: low- and medium-energy x rays, dosimetry protocol, calibration, ionization chambers, reference dosimetry, relative dosimetry

## TABLE OF CONTENTS

I. INTRODUCTION.....	869	D. Quality assurance of the dosimetry equipment and x-ray tube.....	873
A. Historical review.....	869	1. Ionization chamber.....	873
B. Scope of this document.....	870	2. Electrometer.....	873
C. List of nomenclature, symbols, and units.....	870	3. Tube potential of x-ray generator.....	874
II. RADIATION QUALITY SPECIFICATION AND DETERMINATION.....	871	IV. AIR-KERMA CALIBRATION PROCEDURES..	874
A. Energy ranges considered.....	871	V. FORMALISM.....	874
B. Beam quality specifier.....	871	A. The in-air method: Absorbed dose to water at the surface for low- and medium-energy x rays ( $40 \text{ kV} \leq \text{tube potential} \leq 300 \text{ kV}$ ).....	875
C. Determination of HVL.....	872	B. The in-phantom method: Absorbed dose to water at 2 cm depth in water for medium-energy x rays ( $100 \text{ kV} < \text{tube potential} \leq 300 \text{ kV}$ ).....	875
III. EQUIPMENT.....	872		
A. Phantoms.....	872		
B. Dosimeters.....	872		
C. Electrometers.....	873		

C. Other considerations in the calibration measurement . . . . .	875
1. Ion collection efficiency $P_{\text{ion}}$ . . . . .	875
2. Polarity correction $P_{\text{pol}}$ . . . . .	876
3. End effect $\delta t$ . . . . .	876
4. Electrometer correction ( $P_{\text{elec}}$ ) . . . . .	876
5. Temperature–pressure correction $P_{\text{TP}}$ . . . . .	876
6. Inverse-square consideration for in-air calibration with close-ended cones . . . . .	876
7. Method for determination of $P_{\text{stem,air}}$ . . . . .	876
8. Method for in-phantom calibration of chambers not listed in this protocol . . . . .	877
D. Consistency between the in-air method and the in-phantom method . . . . .	877
VI. GUIDELINES FOR DOSIMETRY IN OTHER PHANTOM MATERIALS . . . . .	878
VII. GUIDELINES FOR RELATIVE DOSIMETRY AT OTHER POINTS IN WATER . . . . .	878
A. Characteristics of clinical beams . . . . .	878
B. Recommendations for relative dose measurements in water . . . . .	878
C. Electron contamination of clinical beams . . . . .	879
VIII. EVALUATION OF UNCERTAINTIES . . . . .	880
IX. FUTURE CONSIDERATIONS . . . . .	880
ACKNOWLEDGMENTS . . . . .	881
APPENDIX A. THEORETICAL BASIS FOR A CODE BASED ON AIR-KERMA CALIBRATIONS . . . . .	881
A.1. Low-energy x rays (40 kV ≤ tube potential ≤ 100 kV) . . . . .	881
A.2. Medium-energy x rays (100 kV < tube potential ≤ 300 kV) . . . . .	881
APPENDIX B. DETAILS ON CONVERSION AND CORRECTION FACTORS . . . . .	883
B.1. The in-air method for low- and medium-energy x rays . . . . .	883
B.1.1. In-air mass energy-absorption coefficient ratio $[(\bar{\mu}_{\text{en}}/\rho)_{\text{air}}^w]_{\text{air}}$ . . . . .	883
B.1.2. Backscatter factor $B_w$ . . . . .	883
B.1.3. Chamber stem correction factor $P_{\text{stem,air}}$ . . . . .	883
B.2. The in-phantom calibration method for medium-energy x rays . . . . .	886
B.2.1. In-phantom mass energy-absorption coefficient ratio $[(\bar{\mu}_{\text{en}}/\rho)_{\text{air}}^w]_{\text{water}}$ . . . . .	886
B.2.2. Ion-chamber correction factor $P_{Q,\text{cham}}$ . . . . .	887
B.2.3. Sleeve correction factor $P_{\text{sheath}}$ . . . . .	887
B.3. Conversion factors to calculate dose in other biological materials . . . . .	887
APPENDIX C. SUMMARY OF RECOMMENDATIONS AND WORKSHEETS . . . . .	888
C.1. TG-61 Worksheet: Calculating dose to water on the phantom surface . . . . .	890
C.2. TG-61 Worksheet: Calculating dose to water at 2 cm depth in water . . . . .	891

## I. INTRODUCTION

### A. Historical review

Kilovoltage (40–300 kV) x-ray beams continue to be used in radiation therapy and radiobiology. According to a survey conducted in 1995 by American Association of physicists in Medicine (AAPM) Radiation Therapy Committee Task Group 61,<sup>1,2</sup> there is renewed interest in radiotherapy treatment with superficial and orthovoltage x rays, with more x-ray machines being ordered and installed in North America during the last few years.

For the dosimetry procedures, several dosimetry protocols are available for kilovoltage x-ray beam therapy. In 1973 the International Commission for Radiation Units and Measurements (ICRU) Report No. 23<sup>3</sup> recommended “the in-air method” for low-energy photons (tube potential: 40–150 kV) with the backscatter factors taken from the 1961 British Journal of Radiology (BJR) Supplement 10,<sup>4</sup> and “the in-phantom method” for medium-energy x rays (tube potential: 150–300 kV), respectively. In 1981, the National Council on Radiation Protection and Measurements (NCRP) Report No. 69<sup>5</sup> gave a formula to calculate dose to a phantom material at a point in air (with a minimum phantom) for tube potentials 10 kV through the medium-energy range (up to 300 kV). A backscatter factor was needed to calculate dose on the phantom surface. Two years later, the U.K. Hospital Physicist Association (HPA) adopted the same methodology as that used by the ICRU Report No. 23 for low- and medium-energy x-ray beams.<sup>6</sup> For the backscatter factors, the HPA protocol recommended the values from the 1983 BJR Supplement 17.<sup>7</sup> In 1987, the International Atomic Energy Agency (IAEA) code of practice<sup>8</sup> also recommended two different formalisms for low- and medium-energy photons although the beam-quality ranges were slightly different (low energy: tube potential 10–100 kV, medium energy: tube potential 100–300 kV). The backscatter factors were derived from Monte Carlo calculations. The values of the chamber perturbation factor used by the IAEA have been the source of some controversy.<sup>9–16</sup> In 1991, the Institute of Physical Sciences in Medicine Working Party (IPSM)<sup>17</sup> recommended no change in the conversion factor  $F$  given by HPA but gave a new set of backscatter factors which were derived from a combination of more recent Monte Carlo calculations and experimental results. The more recent code of practice of the Institute of Physics and Engineering in Medicine and Biology (IPEMB)<sup>18</sup> published in 1996 and the code of practice of the Netherlands Commission on Radiation Dosimetry (NCS)<sup>19</sup> published in 1997 further incorporated the chamber correction factors that were consistent within 2% with the new IAEA recommendations issued in the second edition of TRS-277.<sup>13</sup>

In North America, a variety of dosimetry procedures have been used in practice, with a combination of conversion and correction factors measured and/or taken from different protocols.<sup>1,2,20</sup> For the last few years, there have been a number of publications concerning this subject leading to the formation of several dosimetry task groups outside North America and new dosimetry protocols for kilovoltage x rays.

The AAPM Radiation Therapy Committee Task Group 61 was set up to evaluate the current situation and to recommend suitable dosimetry procedures for kilovoltage x-ray beam dosimetry for radiotherapy and radiobiology.

## B. Scope of this document

This protocol deals with the dosimetry of kilovoltage x-rays (tube potential: 40–300 kV) for radiotherapy and radiobiology applications. It is an *air-kerma-based* protocol using a calibration of an ionization chamber in air at a standards laboratory. This protocol is valid only when the conditions of charged particle equilibrium are satisfied. The scope of this protocol is fourfold:

- (1) calibration methodology (dosimeter requirements and phantom configurations);
- (2) determination of absorbed dose to water at reference depths in water;
- (3) determination of absorbed dose to water at other depths in water; and
- (4) determination of absorbed dose to other biological materials on the surface.

## C. List of nomenclature, symbols, and units

The following are the symbols used in this document:

$B_w$ : backscatter factor defined, for the reference field size and beam quality, as the ratio of water kerma at the surface of a semi-infinite water phantom to water kerma at that point in the absence of the phantom. It accounts for the effects of phantom scatter for kilovoltage x-ray beams when the “in-air” method is used for the dose determination.

$C_w^{\text{med}}$ : a factor to convert dose from water to a medium *med*, which is dimensionless.

$D_{\text{med},z}$ : absorbed dose to a medium *med* at a depth *z*, expressed in Gy.

$D_{w,z}$ : absorbed dose to water at a depth *z*, expressed in Gy.  
 $g$ : fraction of the energy of secondary electrons that is lost in radiative processes in the medium, which is dimensionless. For low-*Z* materials, it is less than 0.1% for photons below 300 keV.

HVL: half-value layer, defined as the thickness of an absorbing material (usually Al or Cu) necessary to reduce the air-kerma rate to 50% of its original value in an x-ray beam, in narrow beam conditions. Unit of this quantity is “mm Al” for low-energy x rays and “mm Cu” for medium-energy x rays.

HC: homogeneity coefficient, defined as the ratio of the first half-value layer (HVL) thickness to the second HVL thickness of a medium (usually in Al or Cu), which is dimensionless.

$K_{\text{air}}$ : air kerma, expressed in Gy.

$K_{\text{air}}^{\text{in-med}}$ : air kerma in medium *med*, expressed in Gy.

$K_w$ : water kerma, expressed in Gy.

$K_w^{\text{in-med}}$ : water kerma in medium *med*, expressed in Gy.

$M_{\text{raw}}$ : uncorrected electrometer reading. If no sign is indicated, the measurement is made collecting the same charge as during calibration. If a sign (+ or –) is indicated (see Sec.

V C), it is the sign of the charge collected. Unit C (Coulomb) or rdg (electrometer reading).

$M$ : electrometer reading corrected for temperature, pressure, ion recombination, polarity effect and electrometer accuracy. Unit C (Coulomb).

$(\mu_{\text{tr}}/\rho)_{\text{med}}$ : the mass energy-transfer coefficient for a medium *med*. The unit is  $\text{m}^2/\text{kg}$ . The mass energy-transfer coefficient is the average fractional amount of incident photon energy transferred to kinetic energy of charged particles as a result of the photon interactions with the medium. When multiplied by the photon energy fluence ( $\Psi = \Phi \cdot E$ ), where  $\Phi$  is the photon fluence and  $E$  the photon energy, it gives the kerma to the medium. The mass energy-absorption coefficient is related to the mass energy-transfer coefficient by  $(\mu_{\text{en}}/\rho)_{\text{med}} = (\mu_{\text{tr}}/\rho)_{\text{med}}(1 - g)$ . As  $g$  is generally very small it is often ignored for low- and medium-energy x rays, and the mass energy transfer coefficient is used for the mass energy-absorption coefficient. Thus, the kerma is taken as collision kerma, and we do not distinguish collision kerma and kerma in this protocol unless it is needed.

$(\bar{\mu}_{\text{en}}/\rho)_{\text{med}2}^{\text{med}1}$ : the ratio of the mean mass energy-absorption coefficient for medium 2 (*med 2*) to medium 1 (*med 1*), which is dimensionless. Each of the mean values is calculated by averaging the monoenergetic mass energy-absorption coefficients over the photon energy fluence spectrum at the point of interest either in air or at a depth in water. In ionization chamber dosimetry, we usually have medium 1 = air and medium 2 = water, in which case we have  $(\bar{\mu}_{\text{en}}/\rho)_{\text{air}}^w$ , which is used to convert air kerma to water kerma, either free in air or at a depth in water.

$N_K$ : air-kerma calibration factor, for a specified x-ray beam quality. This quantity, when multiplied with the corrected chamber reading, yields air kerma under the conditions that the photon fluence spectrum and angular distributions are the same as that for which the calibration factor has been derived, expressed in  $\text{Gy C}^{-1}$ .

$P$ : air pressure inside ion chamber, in kPa. The reference measurement pressure is  $P_{\text{ref}} = 101.33 \text{ kPa}$  (or 760 mm Hg).

$P_{\text{dis}}$ : displacement correction factor to account for the effects due to the displacement of water by a stemless chamber (i.e., only the air cavity and the chamber wall), which is dimensionless.

$P_{E,\theta}$ : correction factor to account for the effects on the response of a stemless chamber due to the change in photon energy and angular distributions between the calibration (in air) and measurement (in phantom), which is dimensionless.

$P_{\text{pol}}$ : ionization chamber polarity effect correction factor, which is dimensionless.

$P_{Q,\text{cham}}$ : overall correction factor to account for the effects due to the change in beam quality between calibration and measurement and to the perturbation of the photon fluence at the point of measurement by the chamber, and the chamber stem, which is dimensionless.

$P_{\text{sheath}}$ : waterproofing sheath correction factor to account for the effects of the change in photon attenuation and scattering due to the presence of the waterproofing sheath in a water phantom (if present), which is dimensionless.

$P_{\text{stem,air}}$ : stem correction factor to account for the effects of

the change in photon absorption and scattering between the calibration (in air) and the measurement (in air) due to the presence of the chamber stem, which is dimensionless.

$P_{\text{stem,water}}$ : combined stem correction factor to account for the effects of the change in photon absorption and scattering between the calibration (in air) and the measurement (in phantom) due to the presence of the chamber stem, which is dimensionless.

$T$ : temperature, in °C. For the calibration labs in North America, the reference temperature is  $T_{\text{ref}} = 22^\circ\text{C}$ .

$(W/e)_{\text{air}}$ : average energy expended per unit charge of ionization produced in dry air, having the value 33.97 J/C. Note that the “exposure-to-dose-to-air” conversion coefficient derived from this value is  $0.876 \times 10^{-2}$  Gy/R.

$z_{\text{ref}}$ : reference depth in water for dose calibration measurement, in cm.  $z_{\text{ref}} = 0$  for low-energy (up to 100 kV) x-ray beams.  $z_{\text{ref}}$  can be either 0 or 2 cm for medium-energy (100–300 kV) x-ray beams depending on the point of interest.

SSD: source to surface distance, in cm. This is usually a nominal distance because the exact position of the x-ray source focal spot is not well defined.

“In-air method”: calibration method to obtain absorbed dose to water at the surface of a water phantom, based on an in-air measurement using an ion chamber calibrated free in air.

“In-phantom method”: calibration method to obtain absorbed dose to water at 2 cm depth in water, based on an in-water measurement using an ion chamber calibrated free in air.

Use of the term “shall” and “should”: recommendations on reference dosimetry and quality assurance in this protocol have been systematically preceded by the term shall. These recommendations must be followed to insure the accuracy of the absorbed dose determination using the formalisms and dosimetric data provided in this protocol. This term is not used in the sections headed by the term “Guidelines” in which multiple alternatives may exist for the same purpose. “Should” has been used in situations, where a recommended practice may be modified by the user provided that the replacement practice does not compromise the dosimetry accuracy.

## II. RADIATION QUALITY SPECIFICATION AND DETERMINATION

### A. Energy ranges considered

The energy range ( $40\text{ kV} \leq \text{tube potential} \leq 300\text{ kV}$ ) considered in this paper is divided into two regions of clinical and radiobiological relevance:

- (i) “low-energy (or superficial) x rays”: x rays generated at tube potentials lower than or equal to 100 kV and
- (ii) “medium-energy (or orthovoltage) x rays”: x rays generated at tube potentials higher than 100 kV.

Since this protocol allows for the use of the in-air method throughout the entire 40–300 kV energy range, the most im-

portant reason for this division is to specify a lower limit to the medium energy range, below which the in-phantom method shall not be used.

### B. Beam quality specifier

Specification of a kilovoltage x-ray beam requires knowledge of the photon fluence spectrum at the point of interest. The half value layer (HVL) solely or in combination with the tube potential is often used to characterize the spectrum. HVL is specified in terms of “mm Al” for low-energy x rays and “mm Cu” for medium-energy x rays. For convenience, however, “mm Al” may also be used for x-ray beams with tube potentials up to 150 kV (a superficial x-ray unit may have tube potentials from 30 to 150 kV).

The quality of a beam depends on many factors such as tube potential, target angle, target material, window material, and thickness, monitor chamber material and thickness, filtration material and thickness, shape of collimation, and the source-chamber distance. A measurement of HVL may be affected by the details of the experimental setup, the procedures and the energy dependence of the dosimeters used. Section IIC describes the setup for the measurement of HVL.

There are a variety of reports on measured x-ray spectra essentially from the 1960s and the 1970s,<sup>25–28</sup> that apply to clinical as well as calibration and research x-ray setups. As well, various programs have been developed for the calculation of kilovoltage x-ray spectrum and the HVL value based on the calculated spectrum (see Refs. 29 and 34). Detailed information about the target and the target angle, the materials in the beam and their thicknesses are required for accurate HVL calculations. In general, target material, target angle, filtration material and thickness are given by the manufacturers while other factors are poorly known and may differ from the manufacturer’s specifications.

It is generally considered to be insufficient to use only tube potential or HVL to specify a beam.<sup>21</sup> Commonly used clinical beams have been reported to have a wide range of HVL values corresponding to the same tube potential.<sup>1,2</sup> Chamber-related factors, such as  $N_K$  and  $P_{Q,\text{cham}}$ , as well as the detector-independent mass energy-absorption coefficients for water to air and the backscatter factors, can vary for x-ray beams of the same tube potential but different HVL values, and vice versa.<sup>22,23</sup> Although dosimetry data are increasingly derived as a function of both tube potential and HVL,<sup>28</sup> the use of both tube potential and HVL value may not completely resolve the specification problem for all the quantities involved. Moreover, in the context of a protocol, the addition of a quantity in terms of which the data have to be presented increases complexity and the probability of clinical errors. For the specification of mass energy-absorption coefficient ratios for in-phantom dosimetry, a recent investigation has examined the uniqueness of the ratio of ionization at 2 cm to ionization at 5 cm<sup>24</sup> but more work is required to verify the validity of such a beam quality specifier.

In this protocol, we separate the issue of beam quality specification into two main stages. The first stage deals with



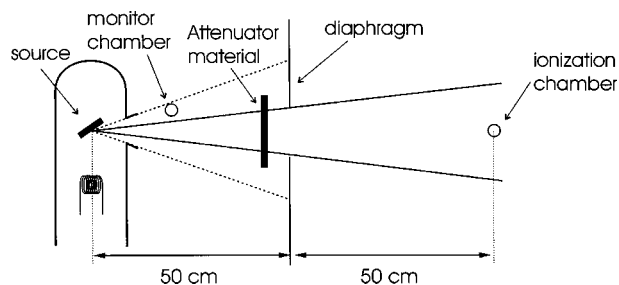


FIG. 1. The experimental setup for HVL measurement. Shown in the figure are source (target), HVL attenuator, diaphragm, and ion chamber. The location of the monitor chamber for normalization of the ion chamber signal, if applicable, is shown. The monitor may already be part of the x-ray setup. If not, it must be positioned such that its response is not affected by changing the filter thickness. The ion chamber for the kerma-rate measurement must be sufficiently energy independent so that a change in filter thickness causes an insignificant change in energy dependence.

obtaining the air-kerma calibration factor  $N_K$  from the standards lab. The chamber shall be calibrated at a beam quality sufficiently close to the user's beam quality in terms of both the tube potential and HVL, to ensure the validity of the calibration factor in the clinical situation (see Sec. III B). Preferably, the chamber should be calibrated at more than one x-ray quality to ensure that the user's beam quality is properly covered. The second stage deals with measuring the absorbed dose in the user beam. At this stage HVL only is considered to be the quality specifier. Section VIII deals with estimates of uncertainties, which include estimates for the lack of complete beam quality specification by using only HVL to specify the quantity involved. For convenience, we only use tube potential to denote the x-ray energy range in this protocol.

### C. Determination of HVL

The first HVL of an x-ray beam is defined as the thickness of a specified attenuator that reduces the air-kerma rate in a narrow beam to one half its original value. The determination of HVL involves the measurement of the variation with the attenuator thickness of air kerma at a point in a scatter-free and narrow beam.<sup>30,31</sup> This means that for this measurement, detectors shall be used with sufficient buildup thickness to eliminate the effect of contaminant electrons (see Sec. III B).

Figure 1 shows the experimental setup for the HVL measurement. The beam diameter defined by the diaphragm shall be 4 cm or less. The thickness of the diaphragm must be thick enough to attenuate the primary beam to 0.1%. The detector shall be placed at least 50 cm away from the attenuating material and the diaphragm. A radiographic check of the alignment of the source, the diaphragm, and the detector shall be performed. A monitor chamber can be used to correct for variations of air-kerma rate especially when the air-kerma rate is significantly lowered by the addition of filtration in the beam during the HVL measurement. In that case, it must be properly placed so that it does not perturb the narrow beam by adding to the scatter component, and its response is not affected by the thickness of the attenuating

material (see Fig. 1). For the air-kerma measurement, small-size detectors are desirable. The beam must cover the sensitive volume of the detector. The detector response shall have limited beam-quality dependence (within 5% between 40 and 300 kV) for accurate HVL measurements. The attenuator shall be made of high-purity (99.9%) material and the thickness of the attenuator shall be measured with an accuracy of 0.05 mm.

## III. EQUIPMENT

### A. Phantoms

When using the in-air method, the measurement is performed free in air, and no phantom is involved (see Sec. V A). When using the in-phantom method (see Sec. V B), water is the phantom material to perform the measurement and the phantom size shall be  $30 \times 30 \times 30 \text{ cm}^3$  or larger. For convenience, plastic phantoms may be used for in-phantom routine quality assurance. However, they shall not be used for in-phantom reference dosimetry for kilovoltage x rays as the chamber correction factors and the conversion factors to derive dose at a depth in water for these phantoms are not well known. In addition, the water equivalence of some commercial plastics for kilovoltage x rays remains an area of active investigation.<sup>33</sup>

### B. Dosimeters

Air-filled ionization chambers shall be used for reference dosimetry in kilovoltage x-ray beams. The effective point of measurement for both cylindrical and parallel-plate chambers is the center of the sensitive air cavity of the chamber. All measurements shall be corrected for temperature, pressure, ion recombination, polarity effect, and electrometer accuracy. The fully corrected reading is defined as  $M = M_{\text{raw}} P_{\text{TP}} P_{\text{ion}} P_{\text{pol}} P_{\text{elec}}$ , where  $M_{\text{raw}}$  is the raw uncorrected reading (in-air or in-phantom). Descriptions of the various correction factors can be found in Sec. V C. Cognizant of chamber response (from either calibration standards laboratories, comparison of known chamber, or manufacturer's data), chamber calibration factors should not vary significantly between two calibration beam qualities so that the estimated uncertainty in the calibration factor for a clinical beam quality between the two calibration qualities is less than or equal to 2%.

For low-energy x rays with tube potentials below 70 kV, calibrated soft x-ray parallel-plate chambers with a thin entrance window shall be used. Thin plastic (low-Z, e.g., polyethylene or PMMA) foils or plates shall be added to the entrance window, if necessary, to remove electron contamination and provide full buildup. When presented for calibration, it is the responsibility of the user to provide these buildup plates or foils as part of their instrument to the Accredited Dosimetry Calibration Laboratories (ADCL), National Institute for Standards and Technology (NIST), or National Research Council of Canada (NRCC), since the same plate or foils are to be used when calibrating the clinical beam. Table I shows total buildup thickness obtained from

TABLE I. Total wall thickness required to provide full buildup and eliminate effects of electron contamination during calibration of a low-energy ( $\leq 100$  kV) clinical beam using thin-window plane-parallel chambers. The window thickness of the chamber (for example,  $2.5 \text{ mg/cm}^2$ ) should be subtracted from the values listed in this table so as to arrive at the required foil or plate thickness for full buildup. The data are calculated from CSDA ranges in polyethylene for the most energetic electrons using ICRU Report No. 37 tabulations (Ref. 42). CSDA ranges in PMMA are about 10% higher. Note that for in-air calibrations in medium-energy x rays ( $>100 \text{ kV}$ ), cylindrical chambers with walls  $>50 \text{ mg/cm}^2$  and without buildup cap shall be used, as their wall thickness is sufficient to provide full buildup.

Tube potential (kV)	Total wall thickness ( $\text{mg cm}^{-2}$ )
40	3.0
50	4.0
60	5.5
70	7.3
80	9.1
90	11.2
100	13.4

the calculated ranges of the most energetic electrons in polyethylene based on continuous-slowing-down approximation (CSDA). The thickness of the needed plate or foils must be determined by subtracting the window thickness (for example,  $2.5 \text{ mg/cm}^2$ ) from the total thickness listed in Table I. For low energy x rays with tube potential of 70 kV or higher, cylindrical chambers that satisfy the chamber response requirements described above can also be used.

Measurements for medium-energy x rays (tube potential 100–300 kV) are performed with the effective point of measurement of the chamber placed either at 2 cm depth in water (in cases where the dose at greater depths is of primary interest) or free in air (in cases where the surface dose is of primary interest). Cylindrical chambers that have a calibration factor varying with the beam quality by less than 3% between 100 and 300 kV shall be used for reference dosimetry. If measurements are performed in water with a nonwaterproof chamber and a waterproofing sleeve, appropriate correction factors shall be applied depending on the sleeve material and thickness (see Appendix B.2.3). Natural or synthetic rubber sleeves shall not be used because their characteristics are unknown for kilovoltage x-ray beams. Care shall be taken that there is no talcum powder involved in waterproofing the chamber, since talcum particles entering the cavity through the venting hole might dramatically change the chamber response.<sup>76</sup> The air gap between chamber and sleeve shall not be larger than 0.2 mm. Cylindrical chambers have adequate thimble thickness ( $50 \text{ mg cm}^{-2}$  or more) and therefore do not require a buildup cap if measurements are done in air.<sup>66</sup>

There have been extensive studies on the correction factors for the commonly used Farmer chamber types for the in-phantom measurement.<sup>10–12,14–16,32</sup> Although in this protocol correction factors are provided for some ionization chambers only (see Appendix B.2.2), other cylindrical chambers matching the above mentioned requirement (i.e., no more than 3% variation of their calibration factor for me-

dium energy x rays) may also be used. However, correction factors must then be determined experimentally by comparing the chambers with a chamber with known correction factors (see Sec. V C.8).

### C. Electrometers

Ionization chambers are read out by the use of a charge- or current-measuring device, normally termed an electrometer. This device shall be capable of reading currents on the order of  $0.01 \text{ nA}$ , with an accumulated charge of  $50\text{--}100 \text{ nC}$ . If calibrated separately from the ionization chamber, the electrometer shall be calibrated by an ADCL, NIST or NRCC and the correction factor applied as part of deriving the corrected ion chamber reading  $M$ . This correction factor is generally close to 1.000 but occasionally can differ from unity by as much as 5%. If the combination of electrometer and ionization chamber is calibrated together as one device no separate electrometer correction is needed (i.e.,  $P_{\text{elec}} = 1$ ).

### D. Quality assurance of the dosimetry equipment and x-ray tube

Quality-assurance procedures shall be performed on all equipment used for the calibration. The major items are listed below:

#### 1. Ionization chamber

A means of monitoring the consistency of the ionization chamber shall be established. This shall be carried out by two or more of the following procedures:

(i) Use of a check source, usually Sr-90: This involves a timed exposure accumulating charge or current measurement. The temperature and pressure corrected chamber reading shall remain consistent within  $\pm 2\%$ . Care must be exercised to ensure that the chamber is placed in the same position each time.

(ii) Redundant chambers: There shall be consistency, to within 2%, in the measurement by using two or more calibrated chambers.

(iii) Use of another beam, such as  $^{60}\text{Co}$ : Establish the baseline response of the chamber at  $^{60}\text{Co}$  and verify the chamber response is reproducible to within 0.2%. Account for the energy dependence of the chamber response, which shall be verified, in the determination of the baseline chamber response at the kV radiation quality of interest. The chamber calibration for medium-energy x rays should be consistent with the  $^{60}\text{Co}$  calibration to within 2%.

The consistency of the response of the ionization chamber shall be checked every time reference dosimetry is accomplished. The chamber shall be checked for constancy before submitting it for calibration to the standards laboratory and rechecked after it is received. The ion chamber shall be calibrated when first purchased, when repaired, when the constancy checks so demand, or once every 2 yr.

#### 2. Electrometer

The electrometer shall be checked along with the ionization chamber using the above procedures. In addition, an-

other calibrated electrometer can be used with the same ionization chamber and should give the same corrected reading to within 0.5%. If the electrometer has a timer feature, charge can be collected for a time interval to determine dose rate. This dose rate shall be the same as that for the x-ray machine timer setting when any end effect, if present, is accounted for (see below).

### 3. Tube potential of x-ray generator

Generally the tube potential will not vary significantly. Consistency of the x-ray output shall be checked routinely. If it changes by more than 3%, the accuracy of settings of the tube potential and filament, including the accuracy and linearity and end effect shall be investigated.<sup>71</sup> This shall also be done as a check on an annual basis.

## IV. AIR-KERMA CALIBRATION PROCEDURES

Implementation of this protocol involves the calibration of the ionization chamber in an appropriate x-ray beam in terms of air kerma free in air ( $K_{\text{air}}$ ) in a standards lab reference beam quality. Suppose that  $K_{\text{air}}$  is the air kerma at the reference point in air for a given beam quality and  $M$  the reading (corrected for temperature, pressure, recombination, polarity effect, and electrometer accuracy) of an ionization chamber to be calibrated with its reference point at the same point. The reference point for plane parallel chambers as well as cylindrical chambers is at the center of the cavity. The field size shall be large enough to provide uniform exposure of the chamber sensitive volume. The air-kerma calibration factor  $N_K$  for this chamber at the specified beam quality is defined as:

$$N_K = \frac{K_{\text{air}}}{M}. \quad (1)$$

The relation between the air kerma and the frequently used exposure calibration factor  $N_X$  is given by

$$N_K = N_X \left( \frac{W}{e} \right)_{\text{air}} (1 - g), \quad (2)$$

where  $(W/e)_{\text{air}}$  has the value  $33.97 \text{ J/C}$  ( $= 0.876 \times 10^{-2} \text{ Gy/R}$ ) for dry air as discussed earlier,  $(1 - g)$  corrects for the effect of radiative losses (mainly due to bremsstrahlung emission) by the secondary charged particles, and  $g$  is less than 0.1% for photons below 300 keV in air.

Calibration factors  $N_K$  shall be traceable to national standards, i.e., from an ADCL, NIST or NRCC, preferably for a number of x-ray beam qualities. **Both tube potential and HVL shall be used to specify the air-kerma calibration factor.** Table II(a) shows some of the x-ray beams as provided by NIST; some ADCLs provide similar beams. Note that a calibration or interpolation between HVLs might be inadequate. For example, depending on the chamber's energy dependence, significant errors may occur if one attempts interpolation between lightly filtered ( $L$  series) beams and medium filtered ( $M$  series) beams. Interpolation may only be per-

TABLE II. (a) Some x-ray beams provided by NIST and the ADCLs for the L and M series. The number part of the beam code represents the tube potential in kV of the beam. (b) Ranges of x-radiation qualities relevant to this protocol provided by NRCC.

(a)	First HVL		Homogeneity coeff. (Al)
	Beam code	(mm Al) (mm Cu)	
L40	0.50		0.59
L50	0.76		0.60
L80	1.83		0.57
L100	2.77		0.57
M20	0.15		0.69
M30	0.36		0.65
M40	0.73		0.69
M50	1.02		0.66
M60	1.68		0.66
M80	2.97		0.67
M100	5.02		0.73
M120	6.79		0.77
M150	10.2	0.67	0.87
M200	14.9	1.69	0.95
M250	18.5	3.2	0.98
M300	22.0	5.3	1.00

(b)	First HVL	
	Peak tube potential	(mm Al) (mm Cu)
40	0.09–2.15	
50	0.09–3.74	
60	0.09–4.89	
70	0.10–5.86	
80	0.10–6.72	
100	0.15–6.83	
120	1.48–8.33	0.09–1.27
135	1.72–8.98	0.10–1.50
150		0.12–1.74
180		0.17–2.18
200		0.21–2.45
250		0.40–3.49
300		0.53–4.57

formed within the same series, e.g., only for the L series or only for the M series. Table II(b) summarizes beam-quality ranges available at NRCC.

The ADCL, NIST, or NRCC may also provide a determination of the ion-collection efficiency during calibration. However, because of the low dose rates used in standards laboratories, this should be generally unity. Ion-collection efficiency is a measure of the fraction of charge measured by the chamber versus the total charge released, and depends on the dose rate and the collecting potential and geometry of the chamber. For the implementation of the protocol, a corrected reading (see Sec. V C) shall be used. The recombination correction can be significant for the calibration of low energy x-ray machines at source to surface distance (SSD) of a few cm where dose rates may be typically on the order of 10 Gy/min at the treatment distance.

## V. FORMALISM

For low-energy x rays (tube potential less than or equal to 100 kV), reference dosimetry shall be performed free in air and a backscatter factor shall be used to account for the



effect of the phantom scatter. For medium-energy x rays (tube potential higher than 100 kV), two different but mutually consistent formalisms can be used. If the point of interest is at the phantom surface ( $z_{\text{ref}}=0$ ), the measurement shall be performed in air and a backscatter factor shall be used to account for the effect of the phantom scatter (the “in-air” method). If the point of interest is at a depth in water, the measurement shall be performed at the reference depth ( $z_{\text{ref}}=2$  cm) in a water phantom and a chamber dependent correction factor (and a waterproofing sheath correction if applicable) shall be applied to account for all differences between the in-air calibration and the measurement in the phantom (the “in-phantom” method).

#### A. The in-air method: Absorbed dose to water at the surface for low- and medium-energy x rays ( $40 \text{ kV} \leq \text{tube potential} \leq 300 \text{ kV}$ )

To use the in-air calibration method for a low- and medium-energy x-ray beam (tube potential: 40–300 kV), the reference depth for the determination of absorbed dose is at the phantom surface ( $z_{\text{ref}}=0$ ). The absorbed dose to water at the phantom surface shall be determined according to

$$D_{w,z=0} = MN_K B_w P_{\text{stem,air}} \left[ \left( \frac{\bar{\mu}_{\text{en}}}{\rho} \right)_{\text{air}}^w \right], \quad (3)$$

where  $M$  is the free-in-air chamber reading, with the center of the sensitive air cavity of the ionization chamber placed at the measurement point ( $z_{\text{ref}}=0$ ), corrected for temperature, pressure, ion recombination, polarity effect, and electrometer accuracy;  $N_K$  the air-kerma calibration factor for the given beam's quality;  $B_w$  the backscatter factor which accounts for the effect of the phantom scatter;  $P_{\text{stem,air}}$  the chamber stem correction factor accounting for the change in photon scatter from the chamber stem between the calibration and measurement (mainly due to the change in field size), and  $[(\bar{\mu}_{\text{en}}/\rho)_{\text{air}}^w]_{\text{air}}$  the ratio for water-to-air of the mean mass energy-absorption coefficients averaged over the incident photon spectrum. The numerical values of the conversion and correction factors in Eq. (3) are discussed in Appendix B.1.

$P_{\text{stem,air}}$  is taken as unity if, for a given beam quality, the same field size is used in the calibration and the measurement. Otherwise, the guidelines in Sec. VC.7 shall be followed to establish  $P_{\text{stem,air}}$ .

The backscatter factor  $B_w$  must include the effect of end plates in close ended cones, if used, on the determination of water kerma at the phantom surface. We have provided a table with multiplicative corrections to the open cone values in Appendix B.1.2.

It shall be remembered that Eq. (3) yields the absorbed dose at the phantom surface under the conditions of charged particle equilibrium and in the absence of electron contamination from the primary beam (i.e., assuming dose=kerma, see Appendix A.1). This applies to open cones as well as to closed cones. For some practical guidelines to deal with electron contamination in clinical beams see Sec. VII C.

The measurement is performed at the point where dose at the phantom surface is required (e.g., the cone end). If this is not possible, the measurement shall be performed at a point as close as possible to the point of interest, and corrected to obtain the dose there. To this end, an inverse square correction can be used (see Sec. VC.6).

#### B. The in-phantom method: Absorbed dose to water at 2 cm depth in water for medium-energy x rays ( $100 \text{ kV} < \text{tube potential} \leq 300 \text{ kV}$ )

This method requires placing a calibrated ionization chamber at a reference depth in a water phantom. If the reference depth is too small there may not be enough buildup material in the upstream direction to cover the whole chamber. If the reference depth is much larger than 2 cm, the ionization signal in the chamber may be too small. Therefore, this protocol has adopted a reference depth of 2 cm. Although the conversion and correction factors needed in the formalism are only slightly dependent on depth, the data provided in this protocol assume a reference depth of 2 cm.

The absorbed dose to water at the 2 cm reference depth ( $z_{\text{ref}}=2$  cm) in water for a  $10 \times 10 \text{ cm}^2$  field defined at 100 cm SSD shall be determined using

$$D_{w,z=2 \text{ cm}} = MN_K P_{Q,\text{cham}} P_{\text{sheath}} [(\bar{\mu}_{\text{en}}/\rho)_{\text{air}}^w]_{\text{water}}, \quad (4)$$

where  $M$  is the chamber reading, with the center of the air cavity of the chamber placed at the reference depth, corrected for temperature, pressure, ion recombination, the polarity effect and electrometer accuracy, and  $N_K$  the air-kerma calibration factor for the given beam's quality [see Eq. (1)].  $P_{Q,\text{cham}}$  is the overall chamber correction factor that accounts for the change in the chamber response due to the displacement of water by the ionization chamber (air cavity plus wall) and the presence of the chamber stem, the change in the energy, and angular distribution of the photon beam in the phantom compared to that used for the calibration in air.  $P_{\text{sheath}}$  is the correction for photon absorption and scattering in the waterproofing sleeve (if present) and  $[(\bar{\mu}_{\text{en}}/\rho)_{\text{air}}^w]_{\text{water}}$  the ratio for water-to-air of the mean mass energy-absorption coefficients, averaged over the photon spectrum at the reference point in water in the absence of the chamber. The numerical values of the conversion and correction factors in Eq. (4) are discussed in Appendix B.2.

#### C. Other considerations in the calibration measurement

The following points need to be considered in the calibration measurement of kilovoltage x-ray beams (consult Appendix C for detailed descriptions of the dose calibration measurement):

##### 1. Ion collection efficiency $P_{\text{ion}}$

To determine accurately the dose absorbed in the air in the ionization chamber cavity, the complete collection of the ions formed by the radiation is required. Some of the ions recombine with ions of the opposite charge on their way to the collection electrode and are not collected. Models have



been developed to estimate the true number of ions formed from measurements made with two different voltages.<sup>52</sup> The value is usually obtained by using the normal collecting voltage and half that voltage.<sup>53–55</sup> Although, recent literature suggests many small problems with this procedure, the recent AAPM TG51 protocol<sup>56</sup> as well as this protocol have used the same procedures because the accuracy is expected to be better than 0.5% at normal chamber operating voltages of 300 V or less.<sup>56</sup> For the procedure, let  $V_H$  be the normal collecting voltage for the detector,  $M_{\text{raw}}^H$  be the raw chamber reading with bias  $V_H$ , and  $M_{\text{raw}}^L$  the raw chamber reading at bias  $V_L$ , where  $V_L/V_H \leq 0.5$ .  $M_{\text{raw}}^L$  and  $M_{\text{raw}}^H$  are to be measured once the chamber readings have reached equilibrium. For continuous beams, the two-voltage approach yields<sup>56</sup>

$$P_{\text{ion}}(V_H) = \frac{1 - \left(\frac{V_H}{V_L}\right)^2}{\frac{M_{\text{raw}}^H}{M_{\text{raw}}^L} - \left(\frac{V_H}{V_L}\right)^2}. \quad (5)$$

Generally  $P_{\text{ion}}$  is close to unity but care should be exercised when using small SSDs. If an ion chamber exhibits a correction factor  $P_{\text{ion}}$  greater than 1.05, the uncertainty becomes unacceptably large and another ion chamber with a smaller recombination effect shall be used.<sup>56</sup>

## 2. Polarity correction $P_{\text{pol}}$

Polarity effects depend on beam quality and cable arrangement and shall be measured and corrected for. The  $P_{\text{pol}}$  factor can be deduced from<sup>56</sup>

$$P_{\text{pol}} = \frac{M_{\text{raw}}^+ - M_{\text{raw}}^-}{2M_{\text{raw}}}, \quad (6)$$

where  $M_{\text{raw}}^+$  is the reading when positive charge is collected,  $M_{\text{raw}}^-$  is the reading when negative charge is collected, and  $M_{\text{raw}}$  (one of  $M_{\text{raw}}^+$  and  $M_{\text{raw}}^-$ ) is the reading corresponding to the charge collected for the reference dosimetry measurements (the same as used for the chamber calibration). In both cases, the sign of  $M_{\text{raw}}$  must be used and usually  $M_{\text{raw}}^+$  and  $M_{\text{raw}}^-$  have opposite signs unless the background is large. Adequate time must be left after changing the sign of the voltage so that the ion chamber's reading has reached equilibrium.

## 3. End effect $\delta t$

The end effect is defined as the amount of time that is not accounted for by the machine timer mechanism during the x-ray beam delivery. This amount of time usually describes the time difference between when the timer mechanism starts and when the desired mA and kV<sub>p</sub> is achieved, or the finite time required for the shutter to move from the fully closed to the fully open position. A small end effect (0.5–3 s) may play a significant role in the output calibration procedure especially for the small dose range (3 min or less treatment duration). The end effect for an x-ray unit can be **measured using the graphical extrapolation method**. The graphical solution of zero exposure on an exposure versus exposure-

timer plot yields the end effect. The end effect  $\delta t$  can also be derived using a mathematical equation described by Attix<sup>57</sup>

$$\delta t = \frac{M_2 \Delta t_1 - M_1 \Delta t_2}{M_1 - M_2}, \quad (7)$$

where  $M_1$  and  $M_2$  are the chamber readings for exposure time  $\Delta t_1$  and  $\Delta t_2$ , respectively. Coffey<sup>20</sup> shows that the above two methods may give slightly different results as the mathematical equation uses only two points, whereas the graphical method uses the whole time range of clinical interest. To ensure the accuracy of the measured end effect, the graphical method shall be used during the machine commissioning and annual QA. The mathematical method may be used for the monthly QA measurement.

## 4. Electrometer correction ( $P_{\text{elec}}$ )

The device used to read the signal from the ionization chamber requires calibration as part of the instrument calibration process. This calibration is performed at the ADCL or NIST. At NRCC, electrometer and chamber are usually calibrated together, as one instrument.  $P_{\text{elec}}$  represents the calibration factor for the reading device only.

## 5. Temperature–pressure correction $P_{\text{TP}}$

The calibration factor assigned by a standards laboratory to an ionization chamber is based on the mass of gas (air) present in the volume. This mass varies with temperature and pressure when the chamber is open to the atmosphere. Therefore, correction of the amount of charge collected in the chamber must be made to the reference temperature ( $T_{\text{ref}}$  is 22 °C) and pressure [ $P_{\text{ref}}$  is 101.33 kPa (760 mm Hg)]. The correction required for the actual temperature and pressure is

$$P_{\text{TP}} = \frac{P_{\text{ref}}}{P} \frac{(T[^\circ\text{C}] + 273.2)}{(T_{\text{ref}}[^\circ\text{C}] + 273.2)}. \quad (8)$$

## 6. Inverse-square consideration for in-air calibration with close-ended cones

Because of the finite size of an ionization chamber it is often impossible to measure the air kerma directly at the cone end. The inverse-square relation can be used to derive the air kerma value at the cone end using the measured value at an extended distance provided the effective source position is known. The effective source position is generally different from the x-ray focal spot due to photon scattering in the end plate. The effective source position can be determined using measurements made at different distances with the smallest chamber available, and then extrapolating to zero distance to the cone end.<sup>3,50</sup> Note that the  $P_{\text{stem,air}}$  value may change (because of its field-size dependence) if measurements are performed at different distances.

## 7. Method for determination of $P_{\text{stem,air}}$

$P_{\text{stem,air}}$  accounts for the effect of the change in photon scatter from the chamber stem between the calibration in a standards laboratory and the in-air measurement in a user's

beam.  $P_{\text{stem,air}}$  should be measured by intercomparing the chamber with unknown  $P_{\text{stem,air}}$  with a reference chamber for which  $P_{\text{stem,air}}$  is known. Let  $f_u$  be the field size for which the beam needs to be calibrated and  $f_c$  the field size for which the chamber has been calibrated at the standards laboratory. The effective point of measurement of the chamber under study and that of the reference chamber should be placed at the same point in air. The stem correction  $P_{\text{stem,air}}(f_u)$  is determined from the equation:

$$P_{\text{stem,air}}(f_u) = \frac{M(f_c)}{M(f_u)} \frac{M_{\text{ref}}(f_u)}{M_{\text{ref}}(f_c)} P_{\text{stem,air,ref}}(f_u), \quad (9)$$

where  $M(f_c)$  and  $M(f_u)$  represent corrected meter readings for the chamber under study;  $M_{\text{ref}}(f_c)$  and  $M_{\text{ref}}(f_u)$  the corrected meter readings for the reference chamber. The field size can be changed either by changing the cone and keeping the chambers at the same position in space or by measuring at several source–chamber distances using a single cone. The requirements for the reference chamber are the same as formulated for the dosimeters used for reference dosimetry (Sec. III B). However, note that the  $N_K$  value for the reference chamber used for the measurement of  $P_{\text{stem,air}}$  does not need to be known as long as it has been established that the response variation satisfies the requirements formulated in Sec. III B. It is suggested that a Farmer type cylindrical chamber with flat response be used as a reference chamber for the measurement of  $P_{\text{stem,air}}$  of another chamber since it has been established that its stem effect varies by less than 1%.<sup>11,15</sup> It is important that, under all circumstances, the sensitive volumes of the chamber under study as well as the reference chamber for the measurement of  $P_{\text{stem,air}}$  be well covered by the radiation beam: the beam diameter should typically be 50% larger than the sensitive diameter of the chamber.

### 8. Method for in-phantom calibration of chambers not listed in this protocol

For a chamber not listed in Appendix B.2.2 the chamber shall be intercompared in-phantom, in the beam of interest, with one of the listed chamber types. To this end, both the investigated chamber and the reference chamber with known air-kerma calibration factor and correction factors should be exposed in-phantom. Irradiation of the investigated chamber should be preceded and followed by the irradiation of the reference chamber at each radiation quality for which a calibration factor is needed, so as to ensure machine stability and positioning reproducibility of the chambers. The point of measurement of both the chamber to be investigated as well as the reference chamber should be placed at the same reference depth. All measurements should be normalized to a monitor chamber reading placed in a position where it does not affect the reading of the reference chamber or the chamber under study (for example, in the phantom downstream in the corner of the field). The overall calibration and correction factor for the investigated chamber can be calculated using:

$$(N_K P_{\text{sheath}} P_{Q,\text{cham}})_u = \frac{M_{\text{ref}}}{M_u} (N_K P_{\text{sheath}} P_{Q,\text{cham}})_{\text{ref}}, \quad (10)$$

where  $M_u$  and  $M_{\text{ref}}$  represent the in-phantom chamber reading of the investigated chamber and the reference chamber, respectively, both corrected for pressure, temperature, ion recombination, and electrometer accuracy, and the other chamber dependent quantities ( $N_K, P_{Q,\text{cham}}, P_{\text{sheath}}$ ) for the reference chamber are provided by the ADCL, NIST, or NRCC, and from this protocol.

### D. Consistency between the in-air method and the in-phantom method

Depth-dose curves for kilovoltage x-ray beams are difficult to measure (and therefore less accurate) especially near the surface. Thus, the determination of the dose on or close to the surface might be less reliable using the in-phantom method compared to the in-air method. If the point of interest is near the surface, the method of choice for calibration for the therapeutic use of kilovoltage x rays is the in-air method. On the other hand, in instances where an accurate dose determination at a depth of 2–3 cm is critical, the point of interest is at a depth and the in-phantom method shall be used. For example, in many animal radiology experiments with large animals such as dogs, pigs, etc., the point of interest is at a depth of several centimeters beneath the skin. The in-phantom method in these cases can provide a more accurate assessment of the dose because the depth-dose curves are more consistent when normalized at 2 cm depth rather than at the surface.

In any case, because of the overlap in methodology in the medium-energy x-ray range, the consistency of the data sets must be ensured. The consistency of using either the in-air or in-phantom method for medium-energy x rays using the data sets in this protocol has been investigated.<sup>34</sup> The procedures for the measurement of the central-axis depth-dose curves, which serve as a link between the dose at the reference depth to the dose elsewhere in a phantom, were examined. Depth-dependent correction factors were calculated using the Monte Carlo method for two types of detectors involved in the measurement of the relative depth-dose curves. Although the two selected detectors differed significantly in their energy responses, after correction, the measured depth-dose curves for both detectors agreed to within 1.5%.<sup>34</sup> Using the corrected depth-dose curves to relate the dose at depth to the dose at the surface, and using the data adopted in this protocol, the consistency between the two methods was within 1% for a 100 kV (2.43 mm Al) beam and within 0.5% for a 300 kV (3.67 mm Cu) beam. It was concluded that the accuracy of the depth-dose measurement was essential to the consistency study. The response of a detector needs to be known accurately before it can be used for depth-dose measurements.

## VI. GUIDELINES FOR DOSIMETRY IN OTHER PHANTOM MATERIALS

This protocol describes methods to determine dose to water at a 2 cm depth in water or at the surface of a water phantom according to the preferred calibration procedure. However, for clinical radiotherapy and radiobiology, the dose to biological tissues on (or near) the irradiated surface is of interest.

The surface dose for other materials (med) can be calculated from

$$D_{\text{med},z=0} = C_w^{\text{med}} D_{w,z=0} \quad (11)$$

with the conversion factor from dose-to-water to dose-to-medium given by

$$C_w^{\text{med}} = \frac{B_{\text{med}}}{B_w} \left[ \left( \frac{\bar{\mu}_{\text{en}}}{\rho} \right)_w^{\text{med}} \right]_{\text{air}}, \quad (12)$$

where  $[(\bar{\mu}_{\text{en}}/\rho)_w^{\text{med}}]_{\text{air}}$  represents the ratio of mass energy-absorption coefficients medium to water averaged over the primary photon spectrum free in air, and  $B_{\text{med}}/B_w$  the ratio of kerma based backscatter factors medium to water. This means that multiplication of  $D_{w,z=0}$  using the procedures described in this protocol with  $C_w^{\text{med}}$  directly gives the dose at the surface of a phantom of material med. The numerical values for the factors in Eq. (12) can be found in Appendix B.3.

## VII. GUIDELINES FOR RELATIVE DOSIMETRY AT OTHER POINTS IN WATER

### A. Characteristics of clinical beams

Prior to the development of this protocol a survey on the status of clinical kilovoltage x-ray dosimetry was carried out.<sup>1,2</sup> In the questionnaire, information was requested on the tube potential and HVL for the radiation qualities in clinical use. Figure 2 shows the relation between tube potential and half value layer as reported by the participants. The wide range of HVL values for the same tube potential reflects the differences in target material and angle, exit window material and thickness, monitor chamber material and thickness, and the variations with filtration material and thickness.

Further information on the characteristics of clinical beams can be found in Jennings and Harrison<sup>43</sup> for x-ray qualities with HVL less than 0.5 mm Cu, and by Smith and Sutherland<sup>44</sup> for HVL of 0.5 mm Cu and higher. Also the papers by Scrimger and Connors,<sup>45</sup> Niroomand-Rad *et al.*,<sup>46</sup> Gerig *et al.*,<sup>47</sup> Kurup and Glasgow,<sup>48</sup> Aukett *et al.*<sup>49</sup> and Li *et al.*<sup>33,50</sup> report on typical characteristics of clinical beams. This material has also been reviewed in BJR Supplement 25.<sup>51</sup>

### B. Recommendations for relative dose measurements in water

The absorbed dose to water at other points in a water phantom can be derived from the measured dose values at

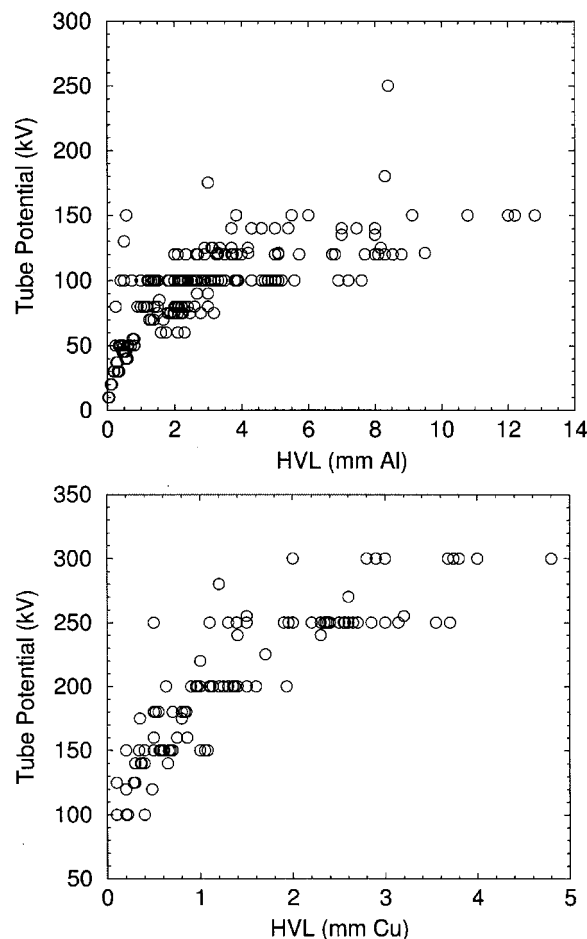


FIG. 2. Relation between tube potential and reported HVL values for low- and medium-energy beams as reported by North American clinics (see Ref. 1).

the reference depth  $z_{\text{ref}}$  and the measured percentage depth dose (PDD) curves. The measurement of PDD and dose profiles is difficult in kilovoltage x-ray beams. **Solid detectors**, attractive because of the small size of their sensitive volume (diode detector, TLD, film), usually show **significant beam-quality dependence** and/or large experimental uncertainties. Well-designed cylindrical chambers have nearly constant energy response for tube potentials between 40 and 300 kV and are suitable for in-phantom measurements. However, the measurement depth is limited to no less than the outer radius of the chamber. Parallel-plate chambers have been used for measurements at smaller depths. Those chambers designed for electron beams usually have a calibration factor varying with beam quality by 20%–40% in kilovoltage x rays. Significant corrections with depth may be required for the PDD measurement with these chambers. Specifically designed thin window chambers for low-energy x rays usually have a flat energy response in air but not at a depth in a phantom. For instance, variations in chamber response of more than 10% have been observed for the Capintec PS-033 chambers. Thus, a depth-dependent correction factor may be required for these chambers to be used in the PDD measurement. Furthermore, the depth dependence of the conversion factor

(from the measured ionization to absorbed dose) may introduce additional uncertainties in the measured percentage depth-dose curves.<sup>22,23</sup>

Although the information on suitable detectors for relative x-ray dosimetry is far from comprehensive, some work has been performed recently to evaluate specific detector types for their suitability to measure depth-dose curves in kilovoltage x-ray beams.<sup>34</sup> As a general requirement to evaluate the suitability of a specific detector, the relative response free in air as well as in-phantom should be compared with a well behaved (Sec. III B) cylindrical chamber at depths where reasonable measurements with the cylindrical chamber can be performed. Diamond detectors and the NACP plane parallel chamber have been found to require relatively small depth dependent corrections in medium-energy x-ray beams<sup>34,58</sup> although one should investigate the specific device in terms of meeting the requirements for accurate relative measurements.<sup>33</sup> Diode detectors are not suitable for relative dosimetry in this photon energy range.

If a suitable detector for relative dosimetry cannot be identified in the clinic the data from the British Journal of Radiology Supplement 25<sup>51</sup> shall be used.

### C. Electron contamination of clinical beams

This paper deals with the determination of the absolute dose at the reference depth ( $z_{\text{ref}}$ ) under the conditions of full charge particle equilibrium, i.e., the dose value is equivalent to the kerma value (see Appendix A). This requires that calibrations and measurements be made using a chamber having enough buildup so that it indeed measures kerma. It is particularly important for the in-air method that the chamber signal is not affected by the contaminating electrons generated in air and on the inside surface of the treatment cone. The presence and specific magnitude of this electron contamination, measured as increased surface dose, depends on the HVL of the x-ray beam, the size of the treatment cone, and the buildup of the chamber (e.g., the window thickness of a parallel-plate chamber) used in the dose determinations.<sup>59–62</sup> It has been further shown<sup>59,62</sup> that this enhanced surface dose depends strongly on the material from which the treatment cone is fabricated with up to a five-fold increase in relative surface dose with lead lined treatment cones (2.0 cm diameter and HVL=3.0 mmCu). Klevenhagen<sup>60</sup> reported that the relative surface dose also changes across the radiation field with the greatest enhanced dose being in the periphery of the treatment field near the edge of the applicator.

In terms of clinical radiation effects, the dose measured at the actual surface of the skin would have little meaning because of the insensitivity of the most superficial skin layers. However, this reported effect may have clinical ramifications depending on the depth of the radiosensitive dermal and epidermal layers of the overlying skin tissues. Epidermal thicknesses have been reported<sup>63</sup> to be 4.7, 6.6 and 40.6 mg/cm<sup>2</sup> on the body trunk, the arms and legs, and the fingertips, respectively. Thus the enhanced radiation dose from electron contamination to the epidermis may be clinically relevant

and should not be ignored. Hence, the ionization chamber window thickness used in surface dose determination discussed above becomes an important issue radiobiologically as well as dosimetrically. The consideration of the high surface dose may be even more important in intracavitary and intraoperative radiotherapy<sup>59,64</sup> in that the irradiated epithelial linings and tissues do not have the insensitive outer layers for protection and any enhanced dose is now given to living cells. To minimize potential radiation overdose to superficial tissues within the treatment field it has been suggested<sup>59,65</sup> that this increase in surface dose can be reduced clinically by: (1) increasing the distance from the applicator cone to the patient surface, (2) inserting an equilibrium thickness of low-Z absorber between the applicator cone and the patient surface, and (3) covering the lead-lined applicator walls with low-Z material of sufficient thickness to achieve equilibrium. Alternatively, the user can measure the extent of the dose enhancement region, if present, by performing measurements with a thin window chamber using plates with thicknesses that provide incomplete buildup, relative to the full buildup situation under which the chamber was calibrated. However, little has been reported in the literature on the factors needed to convert the measured ionization to the dose near the skin surface.

A significant low-energy x-ray dosimetry problem also exists at the interface between two dissimilar materials, e.g., soft tissue and high-Z materials. For example, in some clinical situations, such as treatment of the lip, buccal mucosa, and eyelid lesions, internal shielding is useful to protect the healthy structures beyond the target volume. Lead or some other high-Z material may be used to reduce the transmitted dose to an acceptable level. However, backscattered electrons and photons from the high-Z absorber material will enhance the dose to the surrounding tissues in the immediate vicinity upstream to the shield.

Spiers<sup>66</sup> describes early work on a second, particularly difficult situation in clinical dosimetry presented by soft tissue/bone transition zones encountered with low-energy x rays. The changes in dose which occur at these interface transition zones are difficult to measure and quantify due to the difficulties associated with microscopic distances and the availability of proper dosimetry systems. Saunders and Peters<sup>67</sup> reported this dose enhancement effect for 280 kV orthovoltage x rays. They reported a dose enhancement factor of approximately three near a polystyrene/lead interface, for x rays of 1.7 mm Cu HVL. Wingate *et al.*<sup>68</sup> reported a 1.5–2.2-fold increase in absorbed dose at a one micron distance upstream from a soft tissue/glass interface for superficial and orthovoltage x rays. The dose enhancement fell to a factor of 1.2 at a distance of 5  $\mu\text{m}$  from the interface boundary. Das<sup>69</sup> reported an up to 20-fold localized dose enhancement created by the high-Z interface in kilovoltage (60–240 kV) x-ray beams. Das *et al.*<sup>70</sup> reviewed kilovoltage x-ray dosimetry at high-Z interfaces.

As with the consideration of enhanced surface dose due to photoelectron contamination, the increased dose due to secondary scattered electrons and backscattered photons at the interfaces between soft tissue and high-Z materials may have



TABLE III. Estimated combined standard uncertainty ( $1\sigma$ ) in  $D_w$  at the reference depth in kilovoltage x ray beams using a chamber calibrated in-air in terms of air kerma.

Type of quantity or procedure		Uncertainty (%)
<i>In-air method</i> (for low and medium energies)		
1	$N_K$ from standards laboratory or ADCL	0.7
2	Effect of beam-quality difference between calibration and measurement	2.0
3	Backscatter factor $B_w$	1.5
4	$P_{\text{stem,air}}$	1.0
5	$[(\bar{\mu}_{\text{en}}/\rho)_{\text{air}}^{\text{water}}]_{\text{air}}$	1.5
6	In-air measurement in the user's beam	1.5
	Combined standard uncertainty for $D_{w,z=0}$	<b>3.5</b>
7	Conversion to dose to tissue at the phantom surface	1.0
	Combined standard uncertainty for $D_{\text{tissue},z=0}$	<b>3.6</b>
8	Determination of dose at other points in water	3.0
	Combined standard uncertainty for $D_{w,z}$	<b>4.7</b>
<i>In-phantom method</i> (for medium energies only)		
1	$N_K$ from standards laboratory or ADCL	0.7
2	Effect of beam-quality difference between calibration and measurement	2.0
3	Chamber correction factor $P_{Q,\text{cham}}$	1.5
4	Chamber waterproofing sheath correction factor $P_{\text{sheath}}$	0.5
5	$[(\bar{\mu}_{\text{en}}/\rho)_{\text{air}}^{\text{water}}]_{\text{water}}$	1.5
6	In-water measurement in the user's beam	2.0
	Combined standard uncertainty on $D_{w,z=2\text{ cm}}$	<b>3.6</b>
7	Determination of dose at other points in water	3.0
	Combined standard uncertainty on $D_{w,z}$	<b>4.7</b>

clinical ramifications depending on the total dose prescribed and the radiosensitivity of the surrounding normal tissues. As suggested by Khan<sup>71</sup> for clinical electron beams, one could limit the dose from secondary radiation by coating the upstream side of the high-Z absorber with an adequate thickness low-Z material, i.e., paraffin or other bolus-like material or aluminum.

## VIII. EVALUATION OF UNCERTAINTIES

The final uncertainty in the absorbed dose, which can be delivered to the tumor in a clinical situation, should be better than  $\pm 5\%$ .<sup>77</sup> This final uncertainty comprises several components. The first part occurs as a result of uncertainties in the calibration chain linking the calibration of the clinical beam to the standards laboratory (such as  $N_K$  factor, uncertainties in conversion and correction factors, beam-quality specification uncertainties). The second part is associated with clinical uncertainties in treatment planning dose calculation, patient setup, immobilization, and treatment. The uncertainty discussion here deals only with the former component of the final uncertainty, i.e., the calibration of the clinical beam in terms of the desired quantity (dose to water or dose to tissue). Table III lists the several components contributing to the final uncertainty including type A and type B uncertainties. For a classification of uncertainties we refer to Ref. 8. Consistent with the procedures followed in this report, generally four sources of uncertainties can be considered:

- (i) uncertainties in the air-kerma calibration chain,
- (ii) uncertainties in determining absorbed dose to water at the reference depth in water,
- (iii) uncertainties in determining absorbed dose at other points in water, and
- (iv) uncertainties associated with the transfer of the dose to other biological tissues.

The difference in the uncertainty between the in-air and the in-water measurement (Table III, item 6) is mainly due to the uncertainty in the depth determination. The 1% uncertainty in the air-to-tissue dose conversion for the in-air measurement (Table III, item 7) is mainly due to the uncertainty in the backscatter factor ratio in Eq. (12).

## IX. FUTURE CONSIDERATIONS

The main task of this protocol is to provide recommendations for the determination of absorbed dose to water at the surface or at 2 cm depth in a water phantom irradiated by 40–300 kV x-ray beams under the reference conditions. Guidelines are also provided for the determination of absorbed dose to other biological materials on the surface of a human body and the relative measurement of dose to water at other points in a water phantom for kilovoltage x-ray beams. However, many other clinically related issues, such as those listed below, have not been addressed in this protocol. The following is a brief list of issues, which require further investigation and may be addressed in a future AAPM report:

- (a) determination of absorbed dose to biological tissues at a depth in a human body;
- (b) determination of dose to water using solid phantoms;
- (c) dosimetry for endocavitary radiotherapy (the Papillon technique);
- (d) dosimetry for kilovoltage x-ray radiosurgery systems;
- (e) biological effect of electron contamination;
- (f) biological effect of photon and electron backscattering at tissue/high-Z material interface; and
- (g) relative biological effectiveness (RBE) of kilovoltage x-ray beams.

## ACKNOWLEDGMENTS

We would like to thank the AAPM Radiation Therapy Committee (RTC), especially Jatinder Palta and Jeff Williamson for support and the RTC reviewers Bruce Gerbi, D. W. O. Rogers, Bruce Thomadsen, and other members Julie Dawson, Chris Deibel, John Gibbons, Jr., M. Saiful Huq, Ellen Yorke, and Robert Zwicker for valuable discussions and comments.

## APPENDIX A. THEORETICAL BASIS FOR A CODE BASED ON AIR-KERMA CALIBRATIONS

For kilovoltage x-ray beams, the absorbed dose to water is usually determined with an ionization chamber calibrated in air in terms of air kerma (or exposure). The commonly used ionization chambers are generally considered to be “photon detectors” as the well-known Bragg–Gray cavity theory no longer applies to this energy range.<sup>72</sup>

In order to determine the dose to water, we start with an air-kerma measurement and then convert it to water kerma using the ratio of the mean mass energy-absorption coefficients for water to air, evaluated for the fluence spectrum at the position of interest (free in air or at the reference depth in water). The conversion from water kerma to dose to water is fairly straightforward based on the fact that, for this energy range, the difference between kerma and collision kerma is negligible and the range of the charged particles is small, so that the quasi charged particle equilibrium can be assumed. This is generally true for kilovoltage x-ray beams.

### A.1. Low-energy x rays (40 kV ≤ tube potential ≤ 100 kV)

For low-energy x rays (≤ 100 kV), the measurement is carried out with an ionization chamber free in air, in the absence of any phantoms. The chamber is calibrated in terms of air kerma at a radiation quality sufficiently close to what is present in the user's beam. The air kerma at the point of interest in a user's beam is given by:

$$K_{\text{air}}^{\text{in-air}} = MN_K P_{\text{stem,air}}, \quad (\text{A.1})$$

where  $M$  represents the corrected, free-in-air, ionization chamber reading in the user's beam of the same beam quality and field size as those in the calibration,  $N_K$  the air-kerma calibration factor at the user's beam quality, and  $P_{\text{stem,air}}$  a correction factor accounting for the difference in stem effect

between the calibration beam and the users beam due to the difference in field size between the two beams. This measured air kerma can be converted to water kerma, free in air, through the ratio of mean mass energy-transfer coefficients for water to air  $[(\bar{\mu}_{\text{tr}}/\rho)_{\text{air}}^w]_{\text{air}}$ , evaluated over the photon fluence spectrum free in air, in the absence of a phantom. We then have

$$K_w^{\text{in-air}} = MN_K P_{\text{stem,air}} [(\bar{\mu}_{\text{tr}}/\rho)_{\text{air}}^w]_{\text{air}}. \quad (\text{A.2})$$

Physically,  $K_w^{\text{in-air}}$  represents water kerma to a small mass of water, just large enough to provide full electron buildup, but small enough not to alter the primary photon fluence. The water kerma at the surface of a water phantom  $K_w$  can be calculated using the following relationship:

$$K_w = K_w^{\text{in-air}} B_w, \quad (\text{A.3})$$

where  $B_w$  is the backscatter factor to account for the effect of phantom scatter. Equation (A.3) defines the backscatter factor as the ratio of water kerma at the water surface to water kerma free in air. Generally,  $B_w$  is field size, beam quality and SSD dependent.

The absorbed dose to water  $D_w$  at the water surface can be approximated by  $K_w$  with the assumption of the existence of charged particle equilibrium and the negligible difference between kerma and collision kerma (i.e., assuming  $(\bar{\mu}_{\text{tr}}/\rho)_{\text{air}}^w$  equals  $(\bar{\mu}_{\text{en}}/\rho)_{\text{air}}^w$ ). For this energy range, these assumptions are justified. (Strictly speaking, this approximation is only valid for depths beyond the range of the contaminant electrons and where quasi charged-particle equilibrium has been established.) We then arrive at

$$D_w = M \cdot N_K P_{\text{stem,air}} B_w [(\bar{\mu}_{\text{en}}/\rho)_{\text{air}}^w]_{\text{air}}, \quad (\text{A.4})$$

where  $[(\bar{\mu}_{\text{en}}/\rho)_{\text{air}}^w]_{\text{air}}$  can be calculated from

$$\left[ \left( \frac{\bar{\mu}_{\text{en}}}{\rho} \right)_{\text{air}}^w \right]_{\text{air}} = \frac{\int_0^{E_{\text{max}}} \left( \frac{\mu_{\text{en}}}{\rho}(E) \right)_w E \Phi_E^{\text{free-air}}(E) dE}{\int_0^{E_{\text{max}}} \left( \frac{\mu_{\text{en}}}{\rho}(E) \right)_{\text{air}} E \Phi_E^{\text{free-air}}(E) dE}, \quad (\text{A.5})$$

where  $\Phi_E^{\text{free-air}}(E)$  represents the photon fluence spectrum, differential in energy  $E$ , of the incident x-ray beam at the point of interest. Note that  $[(\bar{\mu}_{\text{en}}/\rho)_{\text{air}}^w]_{\text{air}}$  is independent of field size as it is evaluated over the primary beam only.<sup>73</sup>

### A.2. Medium-energy x rays (100 kV < tube potential ≤ 300 kV)

For medium-energy x-ray beams (tube potential 100–300 kV, HVL: 0.1–4 mm Cu), two different algorithms have been recommended by previous dosimetry protocols. For “the in-air method,” the air kerma is measured in air and then converted to dose to water through the ratio of mass energy-absorption coefficient for water to air and a backscat-

ter factor. For “the in-phantom method,” the air kerma at the reference depth ( $= 5$  cm according to ICRU<sup>3</sup> and IAEA<sup>8</sup>) in water is measured under the reference conditions and then converted to the absorbed dose at the depth of the center of the chamber in undisturbed water using the ratio of mass energy-absorption coefficient for water to air and other beam-quality- and chamber-related correction factors.

The reason for the ICRU<sup>3</sup> protocol to adopt the “in-phantom” measurement at 5 cm depth for medium-energy x-ray beams results from the fact that it is difficult to make accurate measurements in the regions at or close to the surface of a phantom, and the dose distribution here, unlike at greater depths, is considerably affected by the details of the beam defining system.<sup>3</sup> This was considered to be the reason that the British Journal of Radiology Supplement 11<sup>74</sup> gave two distinct sets of depth-dose tables for “close-ended” applicators and “open diaphragms,” respectively. ICRU Report 23<sup>3</sup> suggested that by normalizing the depth-dose curves at a depth rather than at the surface the differences in the recommended depth-dose curves would be virtually eliminated. The dose values at greater depths were of clinical importance as medium-energy x-ray beams were primarily used for treating deep-seated tumors in the 1970s.<sup>3</sup>

Although most of the dosimetry protocols published since the 1970s adopted the in-phantom method for reference dosimetry for medium-energy x-ray beams, the backscatter method is the most used method for this energy range in the clinical radiotherapy community, especially in North America.<sup>1,2</sup> This may be explained by the fact that orthovoltage beams are used mainly for treating tumors close to the surface of the skin. The primary point of interest is the dose near the surface rather than at greater depths. Another reason is that it is more convenient to do routine calibration free in air than in a water phantom.<sup>75</sup>

It is realized that the dosimeter response to kilovoltage x-ray beams has not been fully investigated, especially when placed in a phantom near the surface. The uncertainty in the percentage depth dose measurement can be very large near the phantom surface, depending on the dosimeters used (see Sec. III B). It is therefore clear that if the primary point of interest is at the phantom surface the in-air method shall be used with the reference depth at the phantom surface in order to reduce the uncertainty in the measured dose. On the other hand, if one is more interested in the dose at a depth (to check the dose at the critical organs) than at the surface, “the in-phantom method” shall be used with the reference depth at 2 cm depth. Better agreement in measured percentage depth dose curves at depths of 1 cm and greater can be achieved when normalized to the values at 2 cm reference depth than normalized to the surface values. In addition, a measurement at 2 cm depth provides more signal than one at 5 cm. These are the main reasons why 2 cm has been chosen here.

When the in-air method is used, the measurement is performed with the chamber free in air and the dose to water at the phantom surface can be calculated from Eq. (A.4). Other reference conditions are the same as described in the previous section.

For the in-phantom measurement, use is made of a chamber, calibrated free in air in terms of air kerma at a radiation quality the same as or sufficiently close to that being used to irradiate the phantom. This chamber is placed at the reference depth  $z_{\text{ref}}$  in a full water phantom irradiated with a reference field of medium-energy x rays. Due to phantom attenuation and scattering, the photon spectral and angular distribution is different from that free in air at which the chamber is calibrated. Therefore, the calibration factor  $N_K$ , which applies to the primary radiation, does not necessarily apply to the situation in the phantom. A correction factor  $P_{E,\theta}$  is introduced to account for the change in calibration factor caused by the change in photon energy  $E$  and angular  $\theta$  distribution. The combined effect of the chamber stem free-in-air and in-phantom is usually accounted for separately using an overall correction factor  $P_{\text{stem,water}}$ .<sup>11,15</sup>

Similarly we introduce the waterproofing sheath correction factor  $P_{\text{sheath}}$ , which accounts for the effect of the plastic sheath to protect a nonwaterproof chamber when used in water.<sup>23</sup> Furthermore, by inserting the chamber in the phantom, an amount of water is displaced by the air cavity and the chamber walls (the volume is equivalent to the outer dimensions of the chamber, excluding the stem since the effect of the stem, if present, has been accounted for separately). An additional correction factor  $P_{\text{dis}}$  is then required to account for the change in air kerma at the point of measurement due to the displacement of water by the chamber.<sup>11,16</sup>

The air kerma at the reference depth  $z_{\text{ref}}$ ,  $K_{\text{air}}^{\text{in-water}}$ , can be calculated by

$$K_{\text{air}}^{\text{in-water}} = M \cdot N_K \cdot P_{E,\theta} \cdot P_{\text{stem,water}} \cdot P_{\text{dis}} \cdot P_{\text{sheath}}, \quad (\text{A.6})$$

where  $M$  is the chamber reading corrected for temperature, pressure, polarity effect, and electrometer accuracy, in the user's beam at depth  $z_{\text{ref}}$  in the water phantom. We now introduce the overall correction factor  $P_{Q,\text{cham}}$  which incorporates all “beam-quality  $Q$  and chamber (cham) dependent” corrections mentioned above, except for the sheath correction  $P_{\text{sheath}}$  since it is not directly related to the individual chamber type.  $P_{Q,\text{cham}}$  is defined as

$$P_{Q,\text{cham}} = P_{E,\theta} \cdot P_{\text{stem,water}} \cdot P_{\text{dis}}. \quad (\text{A.7})$$

Air kerma in water, measured as described above, is converted to water kerma, using mass energy-transfer coefficient ratios water to air,  $[(\bar{\mu}_{\text{tr}}/\rho)_{\text{air}}^w]_{\text{water}}$  averaged over the photon fluence spectrum at the point of interest in the phantom in the absence of the chamber, i.e.,

$$K_w = K_{\text{air}}^{\text{in-water}} \left[ \left( \frac{\bar{\mu}_{\text{tr}}}{\rho} \right)_{\text{air}}^w \right]_{\text{water}}. \quad (\text{A.8})$$

The absorbed dose to water  $D_w$  at the reference depth in water can be approximated by  $K_w$  with the assumption of the existence of quasicharged particle equilibrium and the negligible difference between kerma and collision kerma. We then have

$$D_w \simeq K_w = M \cdot N_K \cdot P_{Q, \text{cham}} \cdot P_{\text{sheath}} [(\bar{\mu}_{\text{en}}/\rho)_{\text{air}}^w]_{\text{water}} \cdot \quad (\text{A.9})$$

As stated above,  $P_{Q, \text{cham}}$  carries the complete chamber dependence in the correction procedure except for the sheath correction, whereas  $[(\bar{\mu}_{\text{en}}/\rho)_{\text{air}}^w]_{\text{water}}$  is a chamber independent conversion factor. However, both factors are field-size and depth dependent.

## APPENDIX B. DETAILS ON CONVERSION AND CORRECTION FACTORS

This Appendix contains the numerical data and procedures necessary to apply the expressions based on in-air measurements for low-energy and medium-energy x-ray dosimetry and for the in-phantom measurements at medium energies.

### B.1. The in-air method for low- and medium-energy x rays

#### B.1.1. In-air mass energy-absorption coefficient ratio $[(\bar{\mu}_{\text{en}}/\rho)_{\text{air}}^w]_{\text{air}}$

Table IV gives the values of the in-air mass energy-absorption coefficient ratios applicable to the low-energy kV x-ray range as a function of HVL in Al and to the medium-energy range as a function of HVL in mm Al and Cu. The values given are from a global fit to data from Seuntjens *et al.*,<sup>28</sup> the IPEMB<sup>18</sup> code of practice, and from Ma and Seuntjens.<sup>35</sup> For simplicity, only HVL is used to specify the beam quality. One should therefore keep in mind that the uncertainty on this quantity is no better than  $\pm 1.5\%$ . All the sources are based on the interaction data published by Hubbell,<sup>36</sup> which are consistent with the more recent data by Hubbell and Seltzer<sup>36(b)</sup> for kilovoltage beams.

#### B.1.2. Backscatter factor $B_w$

For tube potentials 40–300 kV, the values of the water-kerma based backscatter factor  $B_w$  are given in Tables V(a) and V(b) as a function of SSD, field size, and HVL (mm Al for low-energy x rays, and mm Cu for medium-energy x rays). The values are from Grosswendt<sup>37,38</sup> and have been independently checked using the experimental data from Klevenhagen<sup>39</sup> and the Monte Carlo data from Knight and Nahum.<sup>22</sup> Note the large dependence of the backscatter factors on field size in the medium-energy x-ray range. For short SSD (= 10 cm), backscatter factors have been given for beam qualities up to 4 mm Al HVL. Since the backscatter factor is fundamentally a water-kerma ratio, reliable measurements are nontrivial. Therefore, for the application of this protocol, backscatter factors should not be measured in the clinic.

The backscatter factors from Table V apply to open-ended collimators. Close-ended applicators require slightly higher backscatter factors because of scattering in the end plate. Table VI shows the multiplicative correction factors to be applied to the open field values for medium-energy x rays for close-ended cones with a PMMA end plate of 3.2 mm.<sup>51</sup>

TABLE IV. Ratios of average mass energy-absorption coefficients water to air, free in air, to convert air kerma to water kerma as a function of HVL (mm Al) or HVL (mm Cu). The values given are from a global fit to data from Seuntjens *et al.* (Ref. 28), the IPEMB (Ref. 18) code of practice, and from Ma and Seuntjens (Ref. 35).

First HVL		$[(\bar{\mu}_{\text{en}}/\rho)_{\text{air}}^w]_{\text{air}}$
(mm Al)	(mm Cu)	
0.03		1.047
0.04		1.047
0.05		1.046
0.06		1.046
0.08		1.044
0.10		1.044
0.12		1.043
0.15		1.041
0.2		1.039
0.3		1.035
0.4		1.031
0.5		1.028
0.6		1.026
0.8		1.022
1.0		1.020
1.2		1.018
1.5		1.017
2.0		1.018
3.0		1.021
4.0		1.025
5.0		1.029
6.0		1.034
8.0		1.045
	0.1	1.020
	0.2	1.028
	0.3	1.035
	0.4	1.043
	0.5	1.050
	0.6	1.056
	0.8	1.068
	1.0	1.076
	1.5	1.085
	2.0	1.089
	3.0	1.100
	4.0	1.106
	5.0	1.109

#### B.1.3. Chamber stem correction factor $P_{\text{stem,air}}$

$P_{\text{stem,air}}$  accounts for the effect of the change in photon scatter from the chamber stem between the calibration in a standards laboratory and the measurement in a user's beam. The effect of photon scattering from the chamber stem has been included in the calibration factor  $N_K$  for the beam quality and photon field used in the calibration. When the user's beam quality and field size match those used in the calibration, no correction is required for the chamber stem effect. However, if the user's field size is different from that used in the calibration the stem effect correction may be significant. The stem effect correction is well within 1% for Farmer type cylindrical chambers<sup>11,15</sup> if the field size (diameter) differs by less than 50% for field sizes greater than 5 cm diameter. No stem corrections are needed for these chambers (i.e.,  $P_{\text{stem,air}} = 1$ ) provided the chamber response variation satis-



TABLE V. Water kerma based backscatter factors  $B_w$  for a water phantom as a function of field diameter ( $d$ ), radiation quality (HVL), and source surface distance (SSD) between (a) 1.5 and 10 cm and (b) 10 and 100 cm for open-ended cones. The values are from Grosswendt (Refs. 37 and 38) and have been independently checked using the experimental data from Klevenhagen (Ref. 39) and the Monte Carlo data from Knight and Nahum (Ref. 22).

(a)		HVL (mm Al)																					
SSD (cm)	d (cm)	0.04	0.05	0.06	0.08	0.1	0.12	0.15	0.2	0.3	0.4	0.5	0.6	0.8	1.0	1.2	1.5	2.0	3.0	4.0			
1.5	1	1.001	1.005	1.009	1.012	1.014	1.016	1.018	1.021	1.027	1.032	1.035	1.038	1.042	1.045	1.047	1.050	1.055	1.057	1.057			
	2	1.008	1.009	1.011	1.014	1.018	1.020	1.023	1.028	1.037	1.045	1.051	1.056	1.065	1.070	1.074	1.080	1.089	1.097	1.098			
	3	1.008	1.009	1.011	1.014	1.018	1.021	1.024	1.029	1.039	1.049	1.055	1.061	1.071	1.079	1.084	1.091	1.103	1.114	1.116			
	5	1.008	1.009	1.011	1.014	1.018	1.021	1.024	1.029	1.040	1.050	1.057	1.064	1.075	1.084	1.090	1.099	1.112	1.125	1.128			
	10	1.008	1.009	1.011	1.014	1.018	1.021	1.024	1.029	1.041	1.051	1.058	1.065	1.076	1.085	1.092	1.100	1.115	1.129	1.132			
	15	1.008	1.009	1.011	1.014	1.018	1.021	1.024	1.029	1.041	1.051	1.058	1.065	1.076	1.085	1.092	1.100	1.115	1.129	1.133			
	20	1.008	1.009	1.011	1.014	1.018	1.021	1.024	1.029	1.041	1.051	1.058	1.065	1.076	1.085	1.092	1.100	1.115	1.129	1.133			
3	1	1.007	1.008	1.010	1.012	1.014	1.016	1.018	1.021	1.027	1.032	1.035	1.038	1.043	1.046	1.047	1.050	1.055	1.060	1.058			
	2	1.008	1.009	1.011	1.014	1.018	1.021	1.024	1.029	1.040	1.049	1.055	1.061	1.070	1.078	1.083	1.089	1.101	1.111	1.110			
	3	1.008	1.009	1.011	1.014	1.018	1.021	1.025	1.031	1.044	1.056	1.063	1.071	1.083	1.093	1.100	1.109	1.125	1.140	1.142			
	5	1.008	1.009	1.011	1.014	1.018	1.022	1.026	1.033	1.048	1.061	1.069	1.078	1.093	1.106	1.115	1.127	1.147	1.170	1.175			
	10	1.008	1.009	1.011	1.014	1.018	1.022	1.026	1.033	1.048	1.061	1.071	1.081	1.098	1.112	1.122	1.136	1.159	1.188	1.195			
	15	1.008	1.009	1.011	1.014	1.018	1.022	1.026	1.033	1.048	1.061	1.071	1.081	1.098	1.113	1.123	1.137	1.160	1.190	1.198			
	20	1.008	1.009	1.011	1.014	1.018	1.022	1.026	1.033	1.048	1.061	1.071	1.081	1.098	1.113	1.124	1.138	1.161	1.191	1.199			
5	1	1.007	1.008	1.009	1.012	1.014	1.016	1.018	1.021	1.027	1.033	1.036	1.039	1.043	1.046	1.048	1.051	1.056	1.060	1.058			
	2	1.007	1.009	1.011	1.014	1.018	1.022	1.025	1.030	1.041	1.051	1.057	1.063	1.073	1.081	1.086	1.092	1.104	1.115	1.113			
	3	1.007	1.009	1.011	1.015	1.019	1.023	1.027	1.033	1.046	1.058	1.066	1.075	1.088	1.098	1.105	1.115	1.132	1.150	1.152			
	5	1.007	1.009	1.011	1.015	1.019	1.023	1.027	1.035	1.050	1.064	1.074	1.085	1.102	1.116	1.126	1.140	1.163	1.191	1.198			
	10	1.007	1.009	1.011	1.015	1.019	1.023	1.027	1.035	1.051	1.066	1.078	1.090	1.111	1.129	1.141	1.158	1.186	1.228	1.240			
	15	1.007	1.009	1.011	1.015	1.019	1.023	1.027	1.035	1.051	1.066	1.078	1.090	1.112	1.130	1.144	1.161	1.191	1.235	1.250			
	20	1.007	1.009	1.011	1.015	1.019	1.023	1.027	1.035	1.051	1.066	1.078	1.090	1.112	1.130	1.144	1.162	1.192	1.237	1.252			
7	1	1.006	1.007	1.008	1.011	1.014	1.016	1.018	1.021	1.027	1.033	1.035	1.038	1.043	1.046	1.048	1.051	1.056	1.061	1.060			
	2	1.007	1.008	1.010	1.014	1.018	1.022	1.025	1.031	1.042	1.052	1.058	1.065	1.075	1.083	1.088	1.094	1.106	1.119	1.118			
	3	1.007	1.008	1.010	1.014	1.019	1.023	1.027	1.034	1.048	1.060	1.068	1.076	1.090	1.101	1.109	1.119	1.137	1.157	1.157			
	5	1.007	1.008	1.010	1.014	1.019	1.023	1.027	1.035	1.051	1.066	1.076	1.087	1.106	1.123	1.134	1.149	1.173	1.207	1.213			
	10	1.007	1.008	1.010	1.014	1.019	1.023	1.028	1.036	1.053	1.069	1.081	1.093	1.116	1.139	1.154	1.173	1.206	1.256	1.271			
	15	1.007	1.008	1.010	1.014	1.019	1.023	1.028	1.036	1.053	1.069	1.081	1.094	1.118	1.142	1.157	1.179	1.214	1.269	1.288			
	20	1.007	1.008	1.010	1.014	1.019	1.023	1.028	1.036	1.053	1.069	1.081	1.094	1.118	1.142	1.158	1.180	1.215	1.271	1.292			
10	1	1.006	1.007	1.009	1.012	1.014	1.016	1.018	1.022	1.028	1.034	1.036	1.038	1.043	1.046	1.048	1.051	1.055	1.062	1.059			
	2	1.007	1.009	1.011	1.014	1.018	1.022	1.025	1.030	1.042	1.052	1.058	1.064	1.075	1.083	1.088	1.094	1.105	1.120	1.118			
	3	1.007	1.009	1.011	1.015	1.019	1.023	1.027	1.034	1.048	1.060	1.069	1.078	1.092	1.103	1.110	1.120	1.135	1.159	1.161			
	5	1.007	1.009	1.011	1.015	1.019	1.023	1.028	1.036	1.052	1.068	1.079	1.091	1.110	1.126	1.137	1.152	1.177	1.211	1.220			
	10	1.007	1.009	1.011	1.015	1.019	1.023	1.028	1.037	1.055	1.072	1.086	1.100	1.125	1.146	1.161	1.182	1.216	1.270	1.296			
	15	1.007	1.009	1.011	1.015	1.019	1.023	1.028	1.037	1.055	1.072	1.087	1.101	1.128	1.151	1.167	1.189	1.226	1.288	1.321			
	20	1.007	1.009	1.011	1.015	1.019	1.023	1.028	1.038	1.056	1.073	1.088	1.102	1.129	1.153	1.169	1.191	1.228	1.293	1.328			
(b)		HVL (mm Al)																					
SSD (cm)	d (cm)	0.04	0.05	0.06	0.08	0.1	0.12	0.15	0.2	0.3	0.4	0.5	0.6	0.8	1.0	1.2	1.5	2.0	3.0	4.0	5.0	6.0	8.0
10	1	1.006	1.007	1.009	1.012	1.014	1.016	1.018	1.022	1.028	1.034	1.036	1.038	1.043	1.046	1.048	1.051	1.055	1.062	1.059	1.057	1.056	1.053
	2	1.007	1.009	1.011	1.014	1.018	1.022	1.025	1.030	1.042	1.052	1.058	1.064	1.075	1.083	1.088	1.094	1.105	1.120	1.118	1.119	1.110	
	3	1.007	1.009	1.011	1.014	1.018	1.022	1.026	1.033	1.047	1.060	1.069	1.078	1.092	1.103	1.110	1.120	1.135	1.159	1.161	1.161	1.152	
	5	1.007	1.009	1.011	1.015	1.019	1.023	1.028	1.036	1.052	1.068	1.079	1.091	1.110	1.126	1.137	1.152	1.177	1.211	1.220	1.224	1.226	
	10	1.007	1.009	1.011	1.015	1.019	1.023	1.028	1.037	1.055	1.072	1.086	1.100	1.125	1.146	1.161	1.182	1.216	1.270	1.296	1.308	1.314	
	15	1.007	1.009	1.011	1.015	1.019	1.023	1.028	1.037	1.055	1.072	1.087	1.101	1.128	1.151	1.167	1.189	1.226	1.288	1.321	1.336	1.345	
	20	1.007	1.009	1.011	1.015	1.019	1.023	1.028	1.038	1.056	1.073	1.088	1.102	1.129	1.153	1.169	1.191	1.228	1.293	1.328	1.346	1.357	
20	1	1.006	1.007	1.008	1.011	1.014	1.016	1.018	1.022	1.028	1.034	1.036	1.039	1.043	1.046	1.049	1.052	1.057	1.061	1.059	1.058	1.056	1.053
	2	1.006	1.008	1.010	1.014	1.018	1.022	1.025	1.031	1.043	1.053	1.059	1.065	1.075	1.083	1.089	1.095	1.107	1.116	1.118	1.118	1.119	
	3	1.006	1.008	1.010	1.014	1.019	1.024	1.028	1.035	1.049	1.061	1.069	1.077	1.092	1.105	1.112	1.122	1.138	1.158	1.162	1.165	1.167	
	5	1.006	1.008	1.010	1.014	1.019	1.024	1.029	1.037	1.054	1.070	1.080	1.091	1.112	1.131	1.143	1.158	1.183	1.215	1.226	1.234	1.240	
	10	1.006	1.008	1.010	1.014	1.019	1.024	1.029	1.039	1.057	1.074	1.088	1.102	1.129	1.155	1.173	1.196	1.235	1.291	1.317	1.334	1.348	
	15	1.006	1.008	1.010	1.014	1.019	1.024	1.030	1.039	1.058	1.075	1.090	1.104	1.133	1.162	1.182	1.208	1.252	1.321	1.356	1.380	1.401	
	20	1.006	1.008	1.010	1.014	1.019	1.024	1.030	1.039	1.058	1.076	1.091	1.106	1.136	1.165	1.186	1.213	1.258	1.334	1.373	1.402	1.426	
30	1	1.006	1.007	1.008	1.011	1.015	1.017	1.019	1.022	1.027	1.032	1.035	1.038	1.043	1.047	1.050	1.053	1.058	1.063	1.061	1.059	1.057	1.053
	2	1.006	1.008	1.010	1.014	1.018	1.022	1.025	1.031	1.042	1.052	1.058	1.064	1.074	1.084	1.090	1.096	1.108	1.120	1.122	1.122	1.120	1.110
	3	1.006	1.008	1.01																			

TABLE V. (Continued.)

(b)		HVL (mm Al)																					
SSD (cm)	d (cm)	0.04	0.05	0.06	0.08	0.1	0.12	0.15	0.2	0.3	0.4	0.5	0.6	0.8	1.0	1.2	1.5	2.0	3.0	4.0	5.0	6.0	8.0
50	20	1.006	1.008	1.010	1.014	1.019	1.024	1.030	1.039	1.058	1.076	1.091	1.107	1.138	1.169	1.190	1.218	1.265	1.350	1.404	1.428	1.441	1.472
	1	1.006	1.007	1.008	1.011	1.014	1.016	1.018	1.021	1.027	1.033	1.035	1.038	1.042	1.045	1.047	1.051	1.057	1.065	1.062	1.059	1.055	1.052
	2	1.006	1.007	1.009	1.013	1.018	1.022	1.025	1.031	1.043	1.053	1.058	1.064	1.073	1.081	1.087	1.095	1.107	1.121	1.122	1.121	1.119	1.112
	3	1.006	1.007	1.009	1.013	1.018	1.023	1.027	1.034	1.049	1.062	1.070	1.078	1.093	1.106	1.114	1.124	1.142	1.163	1.167	1.169	1.170	1.160
	5	1.006	1.007	1.009	1.013	1.018	1.023	1.028	1.037	1.054	1.070	1.081	1.093	1.113	1.132	1.143	1.159	1.185	1.226	1.235	1.241	1.246	1.242
	10	1.006	1.007	1.009	1.013	1.018	1.023	1.029	1.038	1.057	1.076	1.091	1.106	1.134	1.159	1.177	1.202	1.244	1.309	1.336	1.352	1.363	1.375
	15	1.006	1.007	1.009	1.013	1.018	1.023	1.029	1.039	1.058	1.077	1.093	1.110	1.140	1.169	1.190	1.218	1.265	1.346	1.387	1.411	1.428	1.448
100	20	1.006	1.007	1.009	1.013	1.018	1.023	1.029	1.039	1.058	1.077	1.094	1.110	1.142	1.173	1.195	1.224	1.273	1.363	1.414	1.443	1.463	1.493
	1	1.006	1.007	1.008	1.011	1.014	1.016	1.018	1.022	1.028	1.034	1.036	1.038	1.042	1.044	1.046	1.050	1.056	1.062	1.061	1.059	1.056	1.053
	2	1.006	1.008	1.010	1.014	1.018	1.022	1.025	1.031	1.043	1.053	1.058	1.064	1.072	1.080	1.085	1.094	1.107	1.121	1.122	1.120	1.118	1.112
	3	1.006	1.008	1.010	1.014	1.019	1.023	1.027	1.035	1.050	1.063	1.070	1.078	1.092	1.104	1.112	1.123	1.142	1.163	1.168	1.169	1.170	1.162
	5	1.006	1.008	1.010	1.014	1.019	1.023	1.028	1.037	1.055	1.071	1.082	1.093	1.113	1.131	1.143	1.160	1.188	1.225	1.234	1.240	1.244	1.243
	10	1.006	1.008	1.010	1.014	1.019	1.023	1.029	1.039	1.058	1.077	1.091	1.106	1.134	1.158	1.177	1.202	1.245	1.311	1.334	1.351	1.366	1.381
	15	1.006	1.008	1.010	1.014	1.019	1.023	1.029	1.039	1.059	1.078	1.094	1.110	1.140	1.169	1.190	1.219	1.269	1.354	1.391	1.417	1.440	1.460
200	20	1.006	1.008	1.010	1.014	1.019	1.023	1.029	1.039	1.059	1.078	1.095	1.111	1.143	1.172	1.195	1.226	1.278	1.375	1.419	1.451	1.480	1.508
		HVL (mm Cu)																					
SSD (cm)	d (cm)	0.1	0.2	0.3	0.4	0.5	0.6	0.8	1.0	1.5	2.0	3.0	4.0	5.0									
10	1	1.062	1.057	1.056	1.054	1.052	1.050	1.046	1.043	1.037	1.033	1.026	1.021	1.017									
	2	1.120	1.118	1.119	1.113	1.108	1.106	1.103	1.097	1.081	1.071	1.057	1.046	1.038									
	3	1.159	1.161	1.161	1.155	1.150	1.147	1.143	1.135	1.116	1.102	1.081	1.067	1.054									
	5	1.210	1.224	1.226	1.221	1.217	1.214	1.209	1.199	1.170	1.151	1.122	1.101	1.082									
	10	1.269	1.306	1.316	1.313	1.311	1.310	1.307	1.294	1.254	1.227	1.186	1.154	1.126									
	15	1.287	1.335	1.348	1.348	1.348	1.348	1.347	1.332	1.289	1.260	1.213	1.178	1.146									
	20	1.292	1.344	1.361	1.362	1.362	1.363	1.364	1.349	1.303	1.273	1.225	1.188	1.155									
20	1	1.061	1.058	1.055	1.054	1.053	1.051	1.048	1.045	1.038	1.033	1.024	1.020	1.018									
	2	1.116	1.118	1.119	1.114	1.110	1.107	1.102	1.097	1.084	1.074	1.056	1.046	1.039									
	3	1.158	1.164	1.168	1.161	1.155	1.152	1.147	1.140	1.122	1.107	1.082	1.067	1.057									
	5	1.214	1.232	1.242	1.238	1.233	1.229	1.219	1.209	1.184	1.164	1.127	1.104	1.088									
	10	1.290	1.331	1.352	1.353	1.353	1.349	1.339	1.326	1.291	1.260	1.204	1.168	1.141									
	15	1.320	1.377	1.407	1.412	1.415	1.411	1.403	1.389	1.350	1.316	1.251	1.207	1.174									
	20	1.333	1.397	1.434	1.441	1.447	1.443	1.436	1.421	1.381	1.345	1.278	1.230	1.194									
30	1	1.063	1.060	1.056	1.054	1.052	1.050	1.047	1.044	1.038	1.033	1.024	1.020	1.018									
	2	1.120	1.122	1.119	1.113	1.108	1.105	1.101	1.096	1.084	1.073	1.056	1.046	1.038									
	3	1.164	1.168	1.169	1.161	1.155	1.152	1.146	1.139	1.121	1.107	1.082	1.068	1.055									
	5	1.220	1.242	1.242	1.239	1.235	1.231	1.221	1.211	1.184	1.164	1.130	1.106	1.087									
	10	1.297	1.348	1.363	1.366	1.367	1.360	1.347	1.332	1.292	1.263	1.214	1.177	1.147									
	15	1.330	1.401	1.417	1.429	1.438	1.433	1.422	1.405	1.360	1.327	1.270	1.226	1.189									
	20	1.348	1.426	1.446	1.464	1.478	1.473	1.464	1.446	1.399	1.364	1.302	1.254	1.213									
50	1	1.065	1.059	1.054	1.053	1.052	1.050	1.047	1.045	1.038	1.034	1.025	1.020	1.018									
	2	1.121	1.121	1.118	1.114	1.111	1.108	1.103	1.097	1.084	1.073	1.056	1.047	1.040									
	3	1.163	1.169	1.170	1.163	1.157	1.154	1.148	1.140	1.121	1.106	1.084	1.069	1.057									
	5	1.225	1.240	1.247	1.244	1.240	1.235	1.226	1.214	1.184	1.163	1.131	1.108	1.089									
	10	1.308	1.350	1.367	1.372	1.376	1.371	1.360	1.344	1.304	1.274	1.222	1.184	1.152									
	15	1.345	1.408	1.433	1.443	1.452	1.450	1.446	1.428	1.379	1.346	1.285	1.237	1.195									
	20	1.361	1.439	1.471	1.486	1.499	1.498	1.495	1.478	1.428	1.391	1.325	1.272	1.226									
100	1	1.062	1.059	1.055	1.053	1.052	1.050	1.047	1.045	1.038	1.034	1.025	1.020	1.018									
	2	1.121	1.121	1.117	1.114	1.111	1.108	1.104	1.098	1.085	1.074	1.057	1.047	1.040									
	3	1.163	1.169	1.170	1.165	1.160	1.156	1.150	1.142	1.122	1.107	1.082	1.070	1.057									
	5	1.224	1.239	1.245	1.243	1.241	1.237	1.227	1.217	1.188	1.167	1.132	1.109	1.090									
	10	1.310	1.349	1.370	1.378	1.383	1.378	1.369	1.353	1.311	1.278	1.226	1.188	1.155									
	15	1.353	1.413	1.447	1.456	1.463	1.461	1.458	1.441	1.393	1.356	1.291	1.244	1.204									
	20	1.373	1.446	1.490	1.502	1.513	1.514	1.516	1.499	1.447	1.406	1.334	1.282	1.237									

TABLE VI. Multiplicative correction factors to the backscatter factors listed in Table V for use with close-ended cones as a function of HVL (mm Cu) and field diameter  $d$ . The values are for a 3.2 mm PMMA ( $\rho = 1.19 \text{ g/cm}^3$ ) end plate. The data are derived from BJR Supplement 25 (Ref. 51).

$d$ (cm)	HVL (mm Cu)			
	0.5	1	2	3
4.5	1.006	1.005	1.004	1.004
5.6	1.006	1.006	1.005	1.004
6.8	1.007	1.006	1.006	1.004
7.9	1.008	1.007	1.006	1.005
9.0	1.008	1.008	1.006	1.006
11.3	1.009	1.008	1.007	1.006
13.5	1.009	1.009	1.008	1.007
16.9	1.010	1.010	1.009	1.008
22.6	1.011	1.011	1.009	1.008

TABLE VII. Ratio of average mass energy-absorption coefficients of water to air at 2 cm depth in water, for a  $10 \times 10 \text{ cm}^2$  field size, SSD=50 cm, as a function of first HVL (in mm Cu or mm Al). The data are from Ma and Seuntjens (Ref. 35).

First HVL		
(mm Cu)	(mm Al)	$[(\bar{\mu}_{\text{en}}/\rho)_{\text{air}}^w]_{\text{water}}$
0.1	2.9	1.026
0.2	4.8	1.032
0.3	6.3	1.037
0.4	7.5	1.041
0.5	8.5	1.046
0.6	9.3	1.050
0.8	10.8	1.055
1	12.0	1.060
1.5	14.2	1.072
2	15.8	1.081
3	17.9	1.094
4	19.3	1.101
5	20.3	1.105

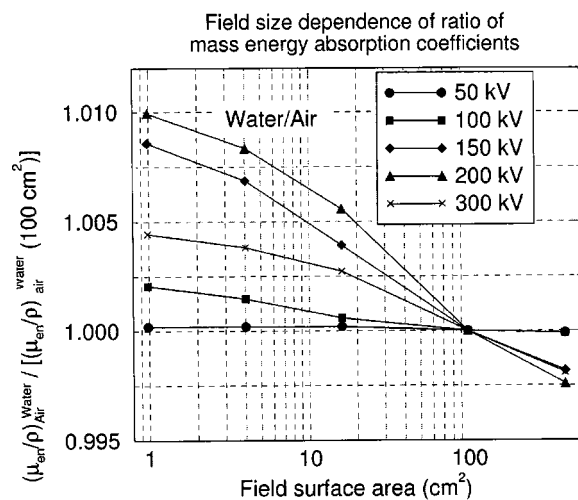


FIG. 3. Dependence on field surface area for different energies of the ratio of the mass energy-absorption coefficient water to air at 2 cm depth in water. Data are normalized to the reference field size of  $10 \times 10 \text{ cm}^2$  at an SSD of 50 cm. Half value layers corresponding to the kV values are: 0.88 mm Al (50 kV), 2.65 mm Al (100 kV), 0.57 mm Cu (150 kV), 1.7 mm Cu (200 kV), and 4.3 mm Cu (300 kV) (see Ref. 35).

TABLE VIII. Overall chamber correction factors  $P_{Q,\text{cham}}$  for common cylindrical chambers in medium-energy x-ray beams. The data applies to 2-cm depth in the phantom, and  $10 \times 10 \text{ cm}^2$  field size. The data are from Seuntjens *et al.* (Ref. 40).

HVL (mm Cu)	Chamber type					
	NE2571	Capintec PR06C	PTW N30001	Exradin A12	NE2581	NE2611 or NE2561
0.10	1.008	0.992	1.004	1.002	0.991	0.995
0.15	1.015	1.000	1.013	1.009	1.007	1.007
0.20	1.019	1.004	1.017	1.013	1.017	1.012
0.30	1.023	1.008	1.021	1.016	1.028	1.017
0.40	1.025	1.009	1.023	1.017	1.033	1.019
0.50	1.025	1.010	1.023	1.017	1.036	1.019
0.60	1.025	1.010	1.023	1.017	1.037	1.019
0.80	1.024	1.010	1.022	1.017	1.037	1.018
1.0	1.023	1.010	1.021	1.016	1.035	1.017
1.5	1.019	1.008	1.018	1.013	1.028	1.014
2.0	1.016	1.007	1.015	1.011	1.022	1.011
2.5	1.012	1.006	1.012	1.010	1.017	1.009
3.0	1.009	1.005	1.010	1.008	1.012	1.006
4.0	1.004	1.003	1.006	1.005	1.004	1.003

## B.2. The in-phantom calibration method for medium-energy x rays

### B.2.1. In-phantom mass energy-absorption coefficient ratio $[(\bar{\mu}_{\text{en}}/\rho)_{\text{air}}^w]_{\text{water}}$

Table VII gives values of  $[(\bar{\mu}_{\text{en}}/\rho)_{\text{air}}^w]_{\text{water}}$  for the medium-energy range at 2 cm depth and a  $10 \text{ cm} \times 10 \text{ cm}$  field size. Figure 3 illustrates the variations of the values of  $[(\bar{\mu}_{\text{en}}/\rho)_{\text{air}}^w]_{\text{water}}$  when the field size differs significantly from the reference field size of  $10 \times 10 \text{ cm}^2$ . The data are from Ma and Seuntjens.<sup>35</sup>

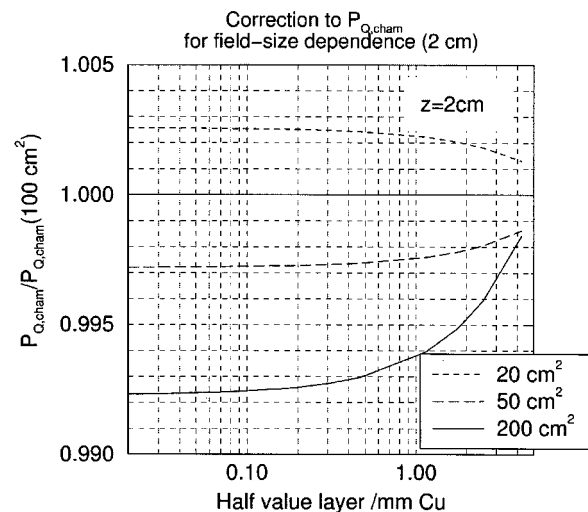


FIG. 4. Field size dependence of  $P_{Q,\text{cham}}$  at the reference depth (2 cm). Correction factor to  $P_{Q,\text{cham}}$  to account for field size dependence for fields significantly differing from the standard  $10 \text{ cm} \times 10 \text{ cm}$ . These values can be applied to all the chambers in Table VIII.

TABLE IX. Water proofing sleeve correction factors  $P_{\text{sheath}}$  for PMMA, polystyrene, and nylon sleeves of thickness  $t$  when using cylindrical chambers for in water phantom measurements in medium-energy x-ray beams. The data applies to 2 cm depth in the phantom, and  $10 \times 10 \text{ cm}^2$  field size. The data are from Ma and Seuntjens (Ref. 23).

HVL		PMMA (Lucite) $\rho = 1.19 \text{ g/cm}^3$				Polystyrene $\rho = 1.06 \text{ g/cm}^3$				Nylon $\rho = 1.14 \text{ g/cm}^3$			
(mm Cu)	(mm Al)	$t = 0.5 \text{ mm}$	$t = 1 \text{ mm}$	$t = 2 \text{ mm}$	$t = 3 \text{ mm}$	$t = 0.5 \text{ mm}$	$t = 1 \text{ mm}$	$t = 2 \text{ mm}$	$t = 3 \text{ mm}$	$t = 0.5 \text{ mm}$	$t = 1 \text{ mm}$	$t = 2 \text{ mm}$	$t = 3 \text{ mm}$
0.1	3.0	0.998	0.995	0.991	0.986	0.995	0.990	0.981	0.972	0.996	0.992	0.985	0.978
0.2	4.7	0.998	0.996	0.993	0.989	0.996	0.993	0.987	0.980	0.997	0.994	0.989	0.984
0.3	6.1	0.998	0.997	0.994	0.991	0.997	0.995	0.989	0.984	0.998	0.995	0.991	0.987
0.4	7.4	0.999	0.997	0.995	0.993	0.998	0.996	0.991	0.987	0.998	0.996	0.993	0.989
0.5	8.5	0.999	0.998	0.996	0.994	0.999	0.996	0.993	0.990	0.999	0.997	0.994	0.992
0.6	9.5	0.999	0.998	0.996	0.995	0.999	0.997	0.994	0.992	0.999	0.997	0.995	0.993
0.8	11.0	0.999	0.998	0.997	0.996	0.999	0.998	0.996	0.994	0.999	0.998	0.996	0.995
1.0	12.1	1.000	0.999	0.998	0.997	1.000	0.999	0.997	0.996	1.000	0.999	0.997	0.996
1.5	13.9	1.000	0.999	0.999	0.999	1.000	0.999	0.998	0.998	1.000	0.999	0.998	0.998
2	15.2	1.000	1.000	1.000	0.999	1.000	0.999	0.999	0.998	1.000	1.000	0.999	0.998
3	17.6	1.000	1.000	1.000	1.000	1.000	0.999	0.999	0.999	1.000	1.000	0.999	0.999
4	19.4	1.000	1.000	1.000	1.000	1.000	1.000	1.000	1.000	1.000	1.000	1.000	1.000
5	20.9	1.000	1.000	1.000	1.000	1.000	1.000	1.000	1.000	1.000	1.000	1.000	1.000

### B.2.2. Ion-chamber correction factor $P_{Q,\text{cham}}$

$P_{Q,\text{cham}}$  accounts for the change in chamber response due to the change in beam characteristics (energy and angular distribution) between calibration and measurement, and of the change in photon fluence at the reference point in the cavity compared to that in water in the absence of the chamber and the chamber stem. Values are derived from measurements and calculations by Seuntjens *et al.*,<sup>11</sup> Ma and Nahum,<sup>14–16</sup> Seuntjens and Verhaegen,<sup>31</sup> and Seuntjens *et al.*<sup>40</sup> Table VIII gives the values of  $P_{Q,\text{cham}}$  for commonly used cylindrical chamber types as a function of HVL. The field-size dependence of this factor at 2 cm depth is 1% or smaller. Figure 4 can be used to estimate this correction to  $P_{Q,\text{cham}}$  if the field size is significantly smaller than  $10 \times 10 \text{ cm}^2$ . The uncertainty of the  $P_{Q,\text{cham}}$  factor was estimated to be about 1.5%.

### B.2.3. Sleeve correction factor $P_{\text{sheath}}$

Table IX gives the values of  $P_{\text{sheath}}$  for sleeves used to insulate cylindrical chambers when placed in a water phantom, as a function of the sleeve thickness  $t$  and HVL. The data are from Monte Carlo calculations and experiments by Ma and Seuntjens.<sup>23</sup> Field-size and SSD dependence of a 1 mm sleeve is less than 0.2% for PMMA, nylon, and polystyrene.<sup>23</sup> The uncertainty of the  $P_{\text{sheath}}$  factor was estimated to be about 0.5%.

## B.3. Conversion factors to calculate dose in other biological materials

This protocol provides guidelines to determine dose to other biological tissues on the surface of a human body for clinical radiotherapy and radiobiology. In this section tables are provided to convert the dose to water to dose to other materials at the surface. The data have been supplied for ICRU four-element soft tissue, ICRU striated muscle, ICRU compact bone, ICRP lung, and ICRP skin. The photon mass-

TABLE X. Free-in-air ratios of mass energy-absorption coefficients of biological tissue to water for application in conjunction with the in-air method. The data are for SSD=50 cm. Except for bone, these values can be used as  $C_w^{\text{med}}$  as defined in Eq. (12). For bone, the data in this table shall be combined with the ratio of backscatter factor bone-to-water as given in Table XI to arrive at  $C_w^{\text{med}}$ . The data are from Ma and Seuntjens (Ref. 35).

“Free-in-air” mass energy-absorption coefficient ratio of the specified tissues to water						
HVL (mm Al) (mm Cu)		ICRU 4- element soft tissue	ICRU striated muscle	ICRP lung	ICRP skin	ICRU compact bone
0.3		0.917	1.016	1.031	0.890	4.200
0.4		0.918	1.020	1.035	0.893	4.289
0.5		0.919	1.022	1.037	0.895	4.335
0.6		0.920	1.024	1.039	0.897	4.382
0.8		0.921	1.028	1.043	0.901	4.475
1.0		0.923	1.031	1.046	0.904	4.494
1.2		0.925	1.031	1.046	0.907	4.469
1.5		0.927	1.032	1.047	0.910	4.427
2.0		0.930	1.032	1.047	0.915	4.350
3.0		0.934	1.032	1.045	0.922	4.179
4.0		0.939	1.030	1.042	0.929	3.975
5.0		0.943	1.028	1.039	0.935	3.769
6.0		0.947	1.026	1.036	0.940	3.557
8.0		0.955	1.021	1.030	0.950	3.133
0.1		0.934	1.032	1.045	0.921	4.209
0.2		0.942	1.029	1.040	0.934	3.808
0.3		0.947	1.026	1.036	0.940	3.561
0.4		0.952	1.023	1.032	0.946	3.314
0.5		0.956	1.020	1.029	0.952	3.068
0.6		0.960	1.018	1.026	0.957	2.859
0.8		0.964	1.015	1.022	0.961	2.657
1.0		0.967	1.012	1.018	0.965	2.456
1.5		0.975	1.006	1.009	0.975	1.952
2.0		0.981	1.001	1.003	0.980	1.637
3.0		0.986	0.996	0.997	0.985	1.280
4.0		0.988	0.994	0.994	0.987	1.128
5.0		0.990	0.992	0.992	0.989	1.026



TABLE XI. Ratios of the kerma-based backscatter factors, bone to water, for photon beams 50–300 kV (0.05–5 mm Cu) with different field sizes at various SSD for Eq. (12). The data are from Ma and Seuntjens (Ref. 35).

SSD (cm)	HVL		$B_{\text{bone}}/B_w$				
	(mm Cu)	(mm Al)	$1 \times 1 \text{ cm}^2$	$2 \times 2 \text{ cm}^2$	$4 \times 4 \text{ cm}^2$	$10 \times 10 \text{ cm}^2$	$20 \times 20 \text{ cm}^2$
10	0.05	1.6	0.958	0.929	0.897	0.861	0.854
	0.1	2.9	0.976	0.945	0.905	0.853	0.838
	0.5	8.5	1.019	1.011	0.974	0.910	0.875
	1	12.0	1.031	1.041	1.026	0.974	0.943
	2	15.8	1.038	1.065	1.077	1.047	1.023
	3	17.9	1.037	1.066	1.092	1.086	1.070
	4	19.3	1.028	1.053	1.082	1.087	1.075
	5	20.3	1.022	1.043	1.074	1.087	1.078
30	0.05	1.6	0.958	0.926	0.889	0.850	0.833
	0.1	2.9	0.976	0.940	0.894	0.837	0.809
	0.5	8.5	1.019	1.011	0.981	0.887	0.833
	1	12.0	1.031	1.042	1.033	0.959	0.902
	2	15.8	1.038	1.067	1.083	1.043	0.989
	3	17.9	1.037	1.067	1.101	1.090	1.047
	4	19.3	1.029	1.055	1.088	1.091	1.065
	5	20.3	1.023	1.045	1.077	1.091	1.079
50	0.05	1.6	0.958	0.927	0.891	0.847	0.827
	0.1	2.9	0.975	0.942	0.897	0.832	0.800
	0.5	8.5	1.018	1.009	0.977	0.881	0.825
	1	12.0	1.031	1.040	1.032	0.958	0.894
	2	15.8	1.038	1.066	1.085	1.047	0.983
	3	17.9	1.036	1.069	1.100	1.095	1.048
	4	19.3	1.028	1.057	1.084	1.094	1.066
	5	20.3	1.022	1.047	1.072	1.094	1.080

energy-absorption coefficient values were taken from Hubbell<sup>36</sup> while the composition of the biological tissues was taken from the ICRU reports.<sup>41,42</sup>

Table X presents ratios of mass energy-absorption coefficients averaged over the photon fluence spectrum free in air of several biological tissues of interest relative to water. The backscatter factor ratios relative to water for any of the tissues (except bone) considered in Table X does not differ from unity by more than 1% for commonly used field sizes and can therefore be ignored.<sup>34</sup> For bone, Table XI shows the ratios of the backscatter factors, bone to water, for photon beams 50–300 kV (0.875–20.8 mm Al) with different field sizes at various SSD.

## APPENDIX C. SUMMARY OF RECOMMENDATIONS AND WORKSHEETS

The following is a summary of the recommendations from this protocol, which is intended to assist the clinical physicist with the measurements in the clinic necessary to complete the Worksheets and hence determine the correct absorbed dose.

(1) Water is the phantom material for absolute dose determination when the point of interest is as a depth of 2 cm for beams of tube potential greater than 100 kV. Plastic phantoms (other than PMMA) may be used for in-phantom routine quality assurance for convenience.

(2) Ionization chambers of choice (Sec. III B): 70–300 kV cylindrical ionization chamber, and 40–70 kV parallel plate (soft x ray) ionization chamber.

The effective point of measurement for both cylindrical and parallel plate chambers is the center of the sensitive air cavity of the chamber.

(3) The appropriate ionization chamber(s) shall be calibrated for at least two beam qualities sufficiently close to, and bracketing the user's beam qualities (in terms of both tube potential and HVL). More than one beam quality is required to ensure that the energy dependence of the chamber response satisfies the requirements enunciated in Sec. III B. Chamber calibration factors shall be directly traceable to national standards (from an ADCL, NIST, or NRCC).

(4) For parallel plate chambers, buildup of appropriate thickness (Table I) and material (polyethylene, PMMA) must be present at the time of ADCL, NIST, or NRCC calibration. Furthermore, for parallel-plate chambers the same buildup materials must be present for all ionization measurements performed at clinical and/or research sites including determination of HVL, reference dosimetry, and chamber evaluation measurements (Sec. III B).

(5) Before ionization data measurements, the clinical physicist shall examine the equipment for appropriate function. This analysis of equipment performance includes the ionization chamber, the electrometer, and the x-ray unit. Spe-

cifically, the x-ray unit shall be assessed for proper functioning of the kV, the mA, and the timer including timer linearity, accuracy, and end effect (Sec. III).

(6) HVL measurements shall be performed with the appropriate chamber (and buildup materials) and in the suggested geometry as indicated in Fig. 1 (Sec. II C).

(7) For energies 40–100 kV, routine dose calibration measurements are performed in air, for energies greater than 100 kV, and depending on the point of interest, dose calibration measurements are performed either in air or at a depth of 2 cm in water. For measurements taken in air, measurements are performed at the point where the dose at the phantom surface is required (e.g., the cone end). If this is not possible, the measurement should be performed at a point as close as possible to the point of interest, and corrected to obtain the dose there. To this end, an inverse square correction can be used (see Sec. V C). For measurements taken in water, the physicist is cautioned on the use of natural or synthetic rubber sleeves for water proofing the chamber because talcum powder particles can enter the chamber and strongly affect the response. PMMA, polystyrene, or nylon shall be used for water protective covering (Sec. III B). The reference point of the parallel plate as well as cylindrical chamber type is at the

center of the sensitive air cavity, along the central axis.

(8) All ionization chamber measurements  $M_{\text{raw}}$  shall be corrected for temperature and pressure, ion recombination, polarity effects, and electrometer calibration effects (Sec. V C).

(9) If the clinical physicist's standard chamber is not included in within the list of chambers in the various correction factor tables, the chamber shall be relatively compared against a chamber, which is included in the respective tables (Sec. V C).

(10) All dose conversion factors and correction factors dependent on energy shall be determined by tabular look-up as a function of the HVL of the user's beam. For in-air measurements, the correction factor of  $P_{\text{stem,air}}$  shall be included in the dose equation (Sec. V A); for in-water measurements the additional correction factors of  $P_{\text{sheath}}$  shall be included in the dose equation (Sec. V B). For  $B_w$  and other correction factors, it is preferred to use the tabular data provided in this paper rather than user-determined experimental values. Unless properly analyzed, user-determined values may contain uncertainties associated with specific assumptions, which are greater than the uncertainties contained within the tabular data (Appendix B).

**C.1. TG-61 Worksheet: Calculating dose to water on the phantom surface****Name:****Date:**

(1) X-ray unit: , Tube potential: kV, HVL: mm (Al or Cu)  
 SSD: cm, Field size: cm<sup>2</sup>

(2) Ion chamber and electrometer calibration. Date of last calibration:

Ion chamber: , Calibration factor  $N_K$  = Gy/C

Electrometer: , Calibration factor  $P_{elec}$  = C/scale unit

(3) Chamber signal:  $M_{raw}$  = scale units

(4) Temperature  $T =$  °C, Pressure  $P$  = kPa  $\left( = \text{mm Hg} \cdot \frac{101.33}{760.0} \right)$

To normalize to 22 °C and 1 atm:

$$P_{TP} = \frac{273.2 + T[^\circ\text{C}]}{295.2} \cdot \frac{101.33}{P[\text{kPa}]} =$$

(5) Total radiation time:  $t =$  min, end effect:  $\delta t$  = min

$$(6) \text{ Recombination correction } P_{ion} = \frac{1 - \left( \frac{V_H}{V_L} \right)^2}{\frac{M_{raw}^H}{M_{raw}^L} - \left( \frac{V_H}{V_L} \right)^2} =$$

$$(7) \text{ Polarity correction } P_{pol} = \left| \frac{M_{raw}^+ - M_{raw}^-}{2M_{raw}} \right| =$$

$$(8) \text{ Corrected chamber reading } M = M_{raw} P_{elec} P_{TP} P_{ion} P_{pol} = \text{C}$$

(9) Backscatter factor (Table V, Table VI):  $B_w =$

(10) Mass energy-absorption coefficient ratio water to air (Table IV):

$$\left[ \left( \frac{\bar{\mu}_{en}}{\rho} \right)_{air}^w \right]_{air} =$$

(11) Stem correction in air (Sec. V C):  $P_{stem,air} =$

$$(12) \text{ Dose to water: } D_w = M N_K B_w P_{stem,air} \left[ \left( \frac{\bar{\mu}_{en}}{\rho} \right)_{air}^w \right]_{air} = \text{Gy}$$

$$(13) \text{ Dose rate: } D_w = \frac{D_w}{t + \delta t} = \text{Gy/min}$$

**C.2. TG-61 Worksheet: Calculating dose to water at 2 cm depth in water****Name:****Date:**

(1) X-ray unit: , Tube potential: kV, HVL: mm (Al or Cu)  
 SSD: cm, Field size: cm<sup>2</sup>

(2) Ion chamber and electrometer calibration. Date of last calibration:

Ion chamber: , Calibration factor  $N_K$  = Gy/C

Electrometer: , Calibration factor  $P_{\text{elec}}$  = C/scale unit

(3) Chamber signal:  $M_{\text{raw}}$  = scale units

(4) Temperature  $T =$  °C, Pressure  $P =$  kPa  $\left( = \text{mm Hg} \cdot \frac{101.33}{760.0} \right)$

To normalize to 22 °C and 1 atm:

$$P_{\text{TP}} = \frac{273.2 + T[^\circ\text{C}]}{295.2} \cdot \frac{101.33}{P[\text{kPa}]} =$$

(5) Total radiation time:  $t =$  min, end effect:  $\delta t =$  min

$$(6) \text{ Recombination correction } P_{\text{ion}} = \frac{1 - \left( \frac{V_H}{V_L} \right)^2}{\frac{M_{\text{raw}}^H}{M_{\text{raw}}^L} - \left( \frac{V_H}{V_L} \right)^2} =$$

$$(7) \text{ Polarity correction } P_{\text{pol}} = \left| \frac{M_{\text{raw}}^+ - M_{\text{raw}}^-}{2M_{\text{raw}}} \right| =$$

(8) Corrected chamber reading  $M = M_{\text{raw}} P_{\text{elec}} P_{\text{TP}} P_{\text{ion}} P_{\text{pol}} =$  C

(9) Chamber correction factor (Table VIII, Fig. 4, Table IX):

$$P_{Q,\text{cham}} P_{\text{sheath}} =$$

(10) Conversion factor (Table VII, Fig. 3):

$$\left[ \left( \frac{\bar{\mu}_{\text{en}}}{\rho} \right)_{\text{air}}^w \right]_{\text{water}} =$$

(11) Dose to water:  $D_w = M N_K P_{Q,\text{cham}} P_{\text{sheath}} \left[ \left( \frac{\bar{\mu}_{\text{en}}}{\rho} \right)_{\text{air}}^w \right]_{\text{water}} =$  Gy

(12) Dose rate:  $D_w = \frac{D_w}{t + \delta t} =$  Gy/min



- <sup>a)</sup>Electronic mail: cma@reyes.stanford.edu
- <sup>b)</sup>Electronic mail: charles.coffey@mcm.vanderbilt.edu
- <sup>c)</sup>Electronic mail: ladewerd@facstaff.wisc.edu
- <sup>d)</sup>Electronic mail: liucr.radonc@shands.ufl.edu
- <sup>e)</sup>Electronic mail: nath@nath1.med.yale.edu
- <sup>f)</sup>Electronic mail: s.seltzer@nist.gov
- <sup>g)</sup>Electronic mail: jseuntjens@medphys.mcgill.ca
- <sup>1</sup>C.-M. Ma, C. W. Coffey, L. A. De Werd, C. Liu, R. Nath, S. M. Seltzer, and J. Seuntjens, "Status of kilovoltage x-ray beam dosimetry in radiotherapy," In *Proceedings of Kilovoltage X-ray Beam Dosimetry for Radiotherapy and Radiobiology*, edited by C.-M. Ma and J. P. Seuntjens (MPP, Madison, 1999), pp. 27–42.
  - <sup>2</sup>C.-M. Ma, C. W. Coffey, L. A. DeWerd, C. Liu, R. Nath, S. M. Seltzer, and J. Seuntjens, "Dosimetry of kilovoltage x-ray beams for radiotherapy," *Med. Phys.* **23** (abstract) (1996).
  - <sup>3</sup>ICRU, "Radiation dosimetry: Measurement of absorbed dose in a phantom irradiated by a single beam of x- or gamma rays," ICRU Report No. 23, ICRU, Washington D.C., 1973 (unpublished).
  - <sup>4</sup>"Central-axis depth-dose data for use in radiotherapy," *Br. J. Radiol.* **10**, (1961).
  - <sup>5</sup>NCRP Report 69, "Dosimetry of x-ray and gamma ray beams for radiation therapy in the energy range 10 keV to 50 MeV," NCRP Publications, Washington DC, 1981 (unpublished).
  - <sup>6</sup>HPA, "Revised code of practice for the dosimetry of 2 to 35 MeV x-ray, and of caesium-137 and cobalt-60 gamma-ray beams," *Phys. Med. Biol.* **28**, 1097–1104 (1983).
  - <sup>7</sup>"Central axis depth dose data for use in radiotherapy," *Br. J. Radiol.* **17**, (1983).
  - <sup>8</sup>IAEA, *Absorbed Dose Determination in Photon and Electron Beams: An International Code of Practice*, Technical Report Series, Vol. 27 (IAEA, Vienna, 1987).
  - <sup>9</sup>U. Schneider, B. Grosswendt, and H. M. Kramer, "Perturbation correction factor for x-rays between 70 and 280 kV," in *Proceedings of the IAEA International Symposium on Dosimetry in Radiotherapy* (IAEA, Vienna, 1988), Vol. I, pp. 141–148.
  - <sup>10</sup>J. Seuntjens, H. Thierens, A. Van der Plaetsen, and O. Segaert, "Determination of absorbed dose to water with ionisation chambers calibrated in free air for medium-energy x-rays," *Phys. Med. Biol.* **33**, 1171–1185 (1988).
  - <sup>11</sup>J. Seuntjens, H. Thierens, and U. Schneider, "Correction factors for a cylindrical chamber used in medium-energy x-ray beams," *Phys. Med. Biol.* **38**, 805–832 (1993).
  - <sup>12</sup>K. E. Rosser, "Measurement of absorbed dose to water for medium-energy x-rays," NPL Report No. RSA(EXT)33, 1992 (unpublished).
  - <sup>13</sup>IAEA, *Absorbed Dose Determination in Photon and Electron Beams: An International Code of Practice*, 2nd ed., Technical Report Series, Vol. 277 (IAEA, Vienna, 1997).
  - <sup>14</sup>C.-M. Ma and A. E. Nahum, "Monte Carlo calculated correction factors for a NE2571 chamber in medium-energy photon beams," in *Proceedings of the IAEA International Symposium on Measurement Assurance in Dosimetry* (IAEA, Vienna, 1994), pp. 371–382.
  - <sup>15</sup>C.-M. Ma and A. E. Nahum, "Monte Carlo calculated stem effect corrections for NE2561 and NE2571 chambers in medium-energy x-ray beams," *Phys. Med. Biol.* **40**, 63–72 (1995).
  - <sup>16</sup>C.-M. Ma and A. E. Nahum, "Calculations of ion chamber displacement effect corrections for medium-energy x-ray dosimetry," *Phys. Med. Biol.* **40**, 45–62 (1995).
  - <sup>17</sup>S. C. Klevenhagen, R. J. Auckett, J. E. Burns, R. M. Harrison, R. T. Knight, A. E. Nahum, and K. E. Rosser, "Report of the IPSM working party on low- and medium-energy x-ray dosimetry," *Phys. Med. Biol.* **36**, 1027–1038 (1991).
  - <sup>18</sup>S. C. Klevenhagen, R. J. Aukett, R. M. Harrison, C. Moretti, A. E. Nahum, and K. E. Rosser, "The IPEMB code of practice for the determination of absorbed dose for x-rays below 300 kV generating potential (0.035 mm Al–4 mm Cu HVL; 10–300 kV generating potential)," *Phys. Med. Biol.* **41**, 2605–2625 (1996).
  - <sup>19</sup>NCS (Netherlands Commission on Radiation Dosimetry), "Dosimetry of low and medium-energy x-rays, a code of practice for use in radiotherapy and radiobiology," NCS Report No. 10, NCS, Delft, The Netherlands, 1997 (unpublished).
  - <sup>20</sup>C. W. Coffey in *Calibrations of Low-energy X-ray units in Advances in Radiation Oncology Physics*, edited by J. Purdy, Medical Physics Monograph 19 (AAPM, New York, 1992), pp. 148–180.
  - <sup>21</sup>J. R. Greening, "The derivation of approximate x-ray spectral distributions and an analysis of x-ray quality specifications," *Br. J. Radiol.* **36**, 363–371 (1960).
  - <sup>22</sup>R. T. Knight and A. E. Nahum, "Depth and field-size dependence of ratios of mass-energy-absorption coefficient, water-to-air, for kV X-ray dosimetry," in *Proceedings of the IAEA International Symposium on Measurement Assurance in Dosimetry* (IAEA, Vienna, 1994), pp. 361–370.
  - <sup>23</sup>C.-M. Ma and J. P. Seuntjens, "Correction factors for water-proofing sleeves in kilovoltage x-ray beams," *Med. Phys.* **24**, 1507–1513 (1997).
  - <sup>24</sup>K. R. Rosser, "An alternative beam quality index for medium-energy x-ray dosimetry," *Phys. Med. Biol.* **43**, 587–598 (1998).
  - <sup>25</sup>E. R. Epp and H. Weiss, "Experimental study of the photon energy spectrum of primary diagnostic x-rays," *Phys. Med. Biol.* **11**, 225–238 (1966).
  - <sup>26</sup>L. H. J. Peaple and A. K. Burt, "The measurement of spectra from x-ray machines," *Phys. Med. Biol.* **14**, 73–85 (1969).
  - <sup>27</sup>W. W. Seelentag, W. Panzer, G. Drexler, L. Platz, and F. Santner, "A catalogue of spectra for the calibration of dosimeters," Report GSF Bericht 560, Gesellschaft für Strahlen- und Umweltforschung GmbH, Munich, 1979 (unpublished).
  - <sup>28</sup>J. Seuntjens, H. Thierens, and O. Segaert, "Response of coaxial Ge(Li) detectors to narrow beams of photons for stripping of x-ray bremsstrahlung spectra," *Nucl. Instrum. Methods Phys. Res. A* **258**, 127–131 (1987).
  - <sup>29</sup>R. Birch and M. Marshall, "Computation of Bremsstrahlung x-ray spectra and comparison with spectra measured with a Ge(Li) detector," *Phys. Med. Biol.* **24**, 505–517 (1979).
  - <sup>30</sup>E. D. Trout, J. P. Kelley, and A. C. Lucas, "Determination of half value layer," *Am. J. Roentgenol.* **84**, 729 (1960).
  - <sup>31</sup>C. A. Carlsson, "Differences in reported backscatter factors for low-energy x-rays: a literature study," *Phys. Med. Biol.* **38**, 521–531 (1993).
  - <sup>32</sup>J. Seuntjens and F. Verhaegen, "Dependence of overall correction factor of a cylindrical ionization chamber on field size and depth in medium-energy x-ray beams," *Med. Phys.* **23**, 1789–1796 (1996).
  - <sup>33</sup>X. A. Li, C.-M. Ma, and D. Salhani, "Measurement of percentage depth dose and lateral beam profile for kilovoltage x-ray therapy beams," *Phys. Med. Biol.* **42**, 2561–2568 (1997).
  - <sup>34</sup>C.-M. Ma, X. A. Li, and J. Seuntjens, "Consistency study on kilovoltage x-ray beam dosimetry for radiotherapy," *Med. Phys.* **25**, 2376–2384 (1998).
  - <sup>35</sup>C.-M. Ma and J. P. Seuntjens, "Mass energy-absorption coefficient and backscatter factor ratios for kilovoltage x-ray beams," *Phys. Med. Biol.* **44**, 131–143 (1999).
  - <sup>36</sup>(a) J. H. Hubbell, "Photon mass attenuation and energy-absorption coefficients from 1 keV to 20 MeV," *Int. J. Appl. Radiat. Isot.* **33**, 1269–1290 (1982); (b) J. H. Hubbell and S. M. Seltzer, "Tables of x-ray mass attenuation coefficients and mass energy-absorption coefficients 1 keV to 20 MeV for elements Z=1 to 92 and 48 additional substances of dosimetric interest," Report No. NISTIR 5632 NIST, Gaithersburg, MD, 1995 (unpublished).
  - <sup>37</sup>B. Grosswendt, "Dependence of the photon backscatter factor for water on source-to-phantom distance and irradiation field size," *Phys. Med. Biol.* **35**, 1233–1245 (1990).
  - <sup>38</sup>B. Grosswendt, "Dependence of the photon backscatter factor for water on irradiation field size and source-to-phantom distance between 1.5 and 10 cm," *Phys. Med. Biol.* **38**, 305–310 (1993).
  - <sup>39</sup>S. C. Klevenhagen, "Experimentally determined backscatter factors for x-rays generated at voltages between 16 and 140 kV," *Phys. Med. Biol.* **34**, 1871–1882 (1989).
  - <sup>40</sup>J. P. Seuntjens, L. Van der Zwan, and C.-M. Ma, "Type dependent correction factors for cylindrical chambers for in-phantom dosimetry in medium-energy x-ray beams," in *Proceedings Kilovoltage X-ray Beam Dosimetry for Radiotherapy and Radiobiology*, edited by C.-M. Ma and J. P. Seuntjens (MPP, Madison, 1999), pp. 159–74.
  - <sup>41</sup>International Commission on Radiation Units and Measurements, *Tissue Substitutes in Radiation Dosimetry and Measurement*, ICRU Report No. 44, Bethesda MD, 1989 (unpublished).
  - <sup>42</sup>International Commission on Radiation Units and Measurements, *Stopping Powers for Electrons and Positrons*, ICRU Report No. 37, Bethesda, MD, 1984.
  - <sup>43</sup>W. A. Jennings and R. M. Harrison, "X rays: HVL range 0.01 to 8.0 mm Al," *Br. J. Radiol.* **17**, 1–22 (1983).

- <sup>44</sup>C. W. Smith and W. H. Sutherland, "X rays: half-value layer range 0.5 mm–4.0 mm Cu," *Br. J. Radiol.* **17**, 23–36 (1983).
- <sup>45</sup>J. W. Scrimger and S. G. Connors, "Performance characteristics of a widely used orthovoltage x-ray therapy unit," *Med. Phys.* **13**, 267–269 (1986).
- <sup>46</sup>A. Niroomand-Rad, M. T. Gillin, F. Lopez, and D. F. Grimm, "Performance characteristics of an orthovoltage x-ray therapy machine," *Med. Phys.* **14**, 874–878 (1987).
- <sup>47</sup>L. Gerig, M. Soubra, and D. Salhani, "Beam characteristics of the Therapax DXT300 orthovoltage therapy unit," *Phys. Med. Biol.* **39**, 1377–1392 (1994).
- <sup>48</sup>R. G. Kurup and G. P. Glasgow, "Dosimetry of a kilovoltage radiotherapy x-ray machine," *Med. Dosim.* **18**, 179–186 (1993).
- <sup>49</sup>R. J. Aukett, D. W. Thoms, A. W. Seaby, and J. T. Gittings, "Performance characteristics of the Pantak DXT-300 kilovoltage x-ray treatment machine," *Br. J. Radiol.* **69**, 726–734 (1996).
- <sup>50</sup>X. A. Li, D. Salhani, and C.-M. Ma, "Characteristics of orthovoltage x-ray therapy beam at extended SSD for applications with end plates," *Phys. Med. Biol.* **42**, 357–370 (1997).
- <sup>51</sup>"Central axis depth dose data for use in radiotherapy," *Br. J. Radiol.* **25**, (1996).
- <sup>52</sup>J. W. Boag, in "Ionization chambers," *Radiation Dosimetry*, edited by F. H. Attix and W. C. Roesch (Academic, New York, 1966), Vol. 2, pp. 1–72.
- <sup>53</sup>J. W. Boag, "General recombination in ionization chambers with spatially non-uniform ionization intensity—two special cases," *Int. J. Radiat. Phys. Chem.* **7**, 243–249 (1975).
- <sup>54</sup>J. W. Boag, in "Ionization chambers," *The Dosimetry of Ionizing Radiation*, edited by K. R. Kase, B. E. Bjarngard, and F. H. Attix (Academic, New York, 1987), Vol. II, pp. 169–244.
- <sup>55</sup>P. R. Almond, "Use of a Victoreen 500 electrometer to determine ionization chamber collection efficiencies," *Med. Phys.* **8**, 901–904 (1981).
- <sup>56</sup>P. R. Almond, P. J. Biggs, B. M. Coursey, W. F. Hanson, M. Saiful-Huq, R. Nath, and D. W. O. Rogers, "AAPM's TG-51 protocol for clinical reference dosimetry of high-energy photon and electron beams," *Med. Phys.* **26**, 1847–1870 (1999).
- <sup>57</sup>F. H. Attix, *Introduction to Radiological Physics and Radiation Dosimetry* (Wiley, New York, 1986), pp. 358–360.
- <sup>58</sup>J. P. Seuntjens, A. H. L. Aalbers, T. W. M. Grimbergen, B. J. Mijnheer, H. Thierens, J. Van Dam, F. W. Wittkamper, J. Zoetelief, M. Piessens, and P. Piret, "Suitability of diamond detectors to measure central axis depth kerma curves for low and medium-energy x-rays," in *Proceedings Kilovoltage X-ray Beam Dosimetry for Radiotherapy and Radiobiology*, edited by C.-M. Ma and J. P. Seuntjens (MPP, Madison, 1999), pp. 227–238.
- <sup>59</sup>M. B. Podgorsak, L. J. Schreiner, and E. B. Podgorsak, "Surface dose in intracavitary orthovoltage radiotherapy," *Med. Phys.* **17**, 635–640 (1990).
- <sup>60</sup>S. C. Klevenhagen, D. D'Souza, and I. Bonnefoux, "Complications in low-energy x-ray dosimetry caused by electron contamination," *Phys. Med. Biol.* **36**, 1111–1116 (1991).
- <sup>61</sup>R. L. Stem and H. D. Kubo, "Considerations for superficial photon dosimetry," *Med. Phys.* **22**, 1469–1470 (1995).
- <sup>62</sup>J. E. Aldrich, J. S. Meng, and J. W. Andrew, "The surface doses from orthovoltage x-ray treatments," *Med. Dosim.* **17**, 69–72 (1992).
- <sup>63</sup>J. T. Whitton, "New values for epidermal thickness and their importance," *Health Phys.* **24**, 1–8 (1973).
- <sup>64</sup>X. A. Li, C.-M. Ma, D. Salhani, and O. Agboola, "Dosimetric evaluation of a widely used kilovoltage x-ray unit for endocavitary radiotherapy," *Med. Phys.* **25**, 1464–1471 (1998).
- <sup>65</sup>L. Ma, C.-M. Ma, J. F. Nacey, and A. L. Boyer, "Determination of cone effects on backscatter factors and electron contamination for superficial x-rays," in *Proceedings Kilovoltage X-ray Beam Dosimetry for Radiotherapy and Radiobiology*, edited by C.-M. Ma and J. P. Seuntjens (MPP, Madison, 1999), pp. 297–290.
- <sup>66</sup>F. W. Spiers, "Transition-zone dosimetry," in *Radiation Dosimetry*, 2nd ed., edited by H. Attix and E. Tochilin (Academic, New York, 1969), pp. 847–850.
- <sup>67</sup>J. E. Saunders and V. G. Peters, "Backscattering for metals in superficial therapy with high energy electrons," *Br. J. Radiol.* **47**, 467–470 (1974).
- <sup>68</sup>C. L. Wingate, W. Gross, and G. Failla, "Experimental determination of absorbed dose from x-rays near the interface of soft tissue and other material," *Radiology* **79**, 984–999 (1962).
- <sup>69</sup>I. J. Das, "Forward dose perturbation at high atomic number interfaces in kilovoltage x-ray beams," *Med. Phys.* **24**, 1781–1792 (1997).
- <sup>70</sup>I. J. Das, J. D. Chapman, F. Verhaegen, and D. E. Zellmer, "Interface dosimetry in kilovoltage photon beams," in *Proceedings of Kilovoltage X-ray Beam Dosimetry for Radiotherapy and Radiobiology*, edited by C.-M. Ma and J. P. Seuntjens (MPP, Madison, 1999), pp. 239–260.
- <sup>71</sup>F. M. Khan, *The Physics of Radiation Therapy*, 2nd ed. (Williams and Wilkins, Baltimore, MD, 1994), pp. 43–44, 394–399.
- <sup>72</sup>C.-M. Ma and A. E. Nahum, "Bragg-Gray theory and ion chamber dosimetry in photon beams," *Phys. Med. Biol.* **36**, 413–428 (1991).
- <sup>73</sup>A. E. Nahum and R. T. Knight, "Consistent formalism for kV x-ray dosimetry," in *Proceedings of the IAEA International Symposium on Measurement Assurance in Dosimetry* (IAEA, Vienna, 1994), pp. 451–459.
- <sup>74</sup>"Central axis depth dose data for use in radiotherapy," *Br. J. Radiol.* **11**, (1972).
- <sup>75</sup>B. Owsley, C. Coffey, and J. Sayeg, "Wall requirements for a thin window parallel plate chamber for the output measurements of a superficial x-ray machine— a forgotten principle?," *Med. Phys.* **17**, 510 (1990).
- <sup>76</sup>W. F. Hanson, D. J. Arnold, R. J. Shalek, and L. J. Humphries, "Contamination of ionization chambers by talcum powder," *Med. Phys.* **15**, 776–777 (1983).
- <sup>77</sup>A. Brahme, "Dosimetric precision requirements in radiation therapy," *Acta Radiol.: Oncol.* **23**, 379–391 (1984).